" LOW LEVEL LIGHT INTENSITIES "

being

A THESIS FOR THE DEGREE OF MASTER OF SCIENCE

of

THE UNIVERSITY OF SYDNEY

by

J. G. CLOUSTON A.S.T.C., B.Sc.

MARCH 1951

FOREWORD

The thesis is based on work carried out under the direction of Mr. P.G. Guest M.Sc. A. Inst. Phys. during 1949 and 1950. For the first twelvemonths the author was an Honours student at the University and for the latter had the help of a Commonwealth Research Grant. The thesis deals with the developement of new techniques for

(a) photoelectrically recording a Stellar Transit

(b) the automatic counting of interference fringes

(c) the photoelectric delineation of the intensity distributions of fringe patterns

and describes a variation of the Michelson interferometer which used as a refractometer will possess certain advantages over existing instruments.

Acknowledgements

It is desired to thank Professor V. A. Bailey sincerely for obtaining sufficient extension of the Commonwealth Research Grant to complete this work. and for permission to present this thesis.

The variety of help and consideration received from different members of the staff and fellow students has been very much appreciated. In particular, the ready co-operation of Mr. Hutchinson and his staff in the machine shop and of Mr. Collins as an Honours student requires special mention.

To Mr. Guest goes the author's deepest gratitude for allowing him to be associated with his very interesting work.

TABLE OF CONTENTS

Chapter I

THE AIM

The ability of the Photomultiplier tube to produce relatively large output currents from small light fluxesmakes the photoelectric recording of stellar transits distinctly possible. For the same reason, the automatic counting of interference fringes becomes feasible. Although its response varies with wavelength so that it does not measure energy directly, it is superior to the photographic plate- microphotometer method of determining intensity distributions. Consequently, with it a more direct approach to their study might be made.

Photographic methods have the definite disadvantage that the blackening of the plate is a complicated function of intensity and exposure time. This necessitates a series of calibration exposures whose intensities are known. In addition, local variations in emulsion sensitivity, non-uniform developement and plate grain place limitations on the precision obtainable with photographic photometry. The simple photocell, the Photomultiplier tube and the Thermocouple, when used with suitable precautions give a response which is linear with respect to intensity, and are capable of giving more precise results than the photographic plate. In point of fact, the Photomutiplier tube has been found to be of great use in Spectroscopy,[I,2,3] where it has been possible by scanning the spectrum to record directly the intensity variations at different wavelengths. Such methods offer particular advantages in the study of Raman spectra[4], where the fact that the parent line is so much more intense than its satellites causes the problem of exposures to be difficult.

The apparently great dissimilarity

between the recording of a stellar transit and the counting of an interference fringe disappears, when considered from the point of view of technique.

In those systems where interference arise from the superposition of two coherent beams the intensity variation of the light is represented by

$$I = 4\,A^2 \cos^2 \delta/2$$

Where A = the amplitude of either wave

= 2π(Path Difference)/λ .

Figure I represents this distribution.

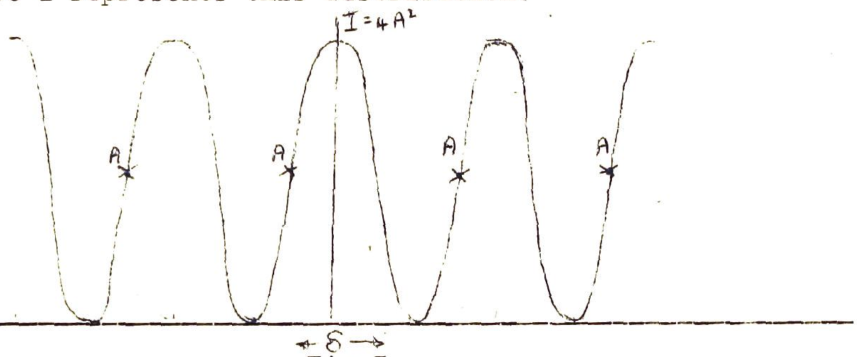

Fig.I

On the other hand the passage of a star across the field of view of a telescope which has several cross hairs in the focal plane of its eyepiece, may be represented by figure 2.

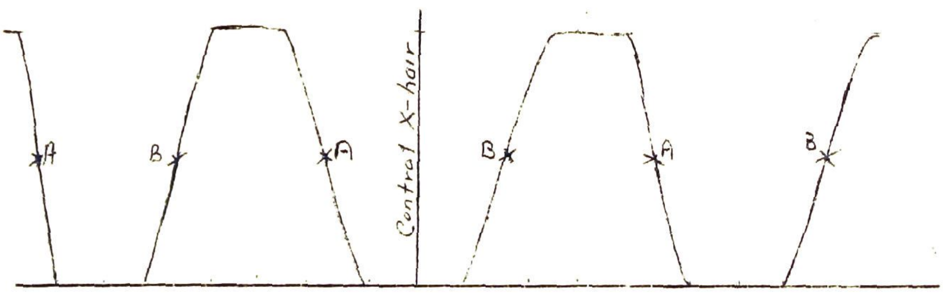

In this case the maximum intensity will be a function of the magnitude of the star and the aperture of the telescope, while the time between successive minima will depend on the declination of the star and the spacing of the cross hairs.

If it could be arranged to have the output of the Photomultiplier trigger a pulse at say A, in figureI, then such a technique would give a count of fringes. On the other hand if a circuit was tripped at both A and B in figure 2 then it would be possible to determine the instant a star was bisected by the cross hair.

Therefore, any attempt to develop these techniques would require some such scheme as is represented in block form by figure 3.

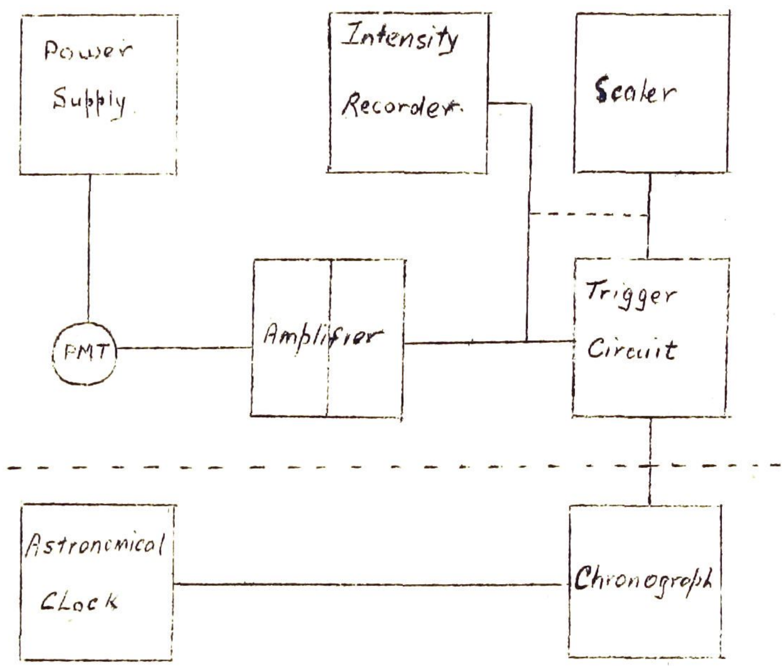

In fringe counting the output of the amplifier might be coupled directly to a chart recorder and the intensity distribution of the fringe system delineated. The pulses from the trigger circuit might be impressed on the record or fed into a scaler. However, the aim with stellar transits would be to record the pulses on a chronograph which simultaneously was receiving signals from an Astronomical clock.

These then are, in outline, the problems. In practice however, the conditions were found to be far from ideal and the difficulties that were struck together with the means taken to overcome them will form the subject matter of subsequent chapters.

CHAPTER II

A. The Electron Multiplier Phototube

Prior to 1936, the phenomenon of secondary emission was studied more from the point of view of reducing its effect than enhancing it. The only practical use to which it had been put was by Hull in the developement of the Dynatron oscillator. In 1936, Zworikin, Malter and Morton[5] published details of a phototube which employed secondary emission to amplify the photocathode current.

Essentially, amplification by secondary emission involves the focussing of the photo-electrons onto an electrode which has been sensitised for secondary emission. The secondary electrons released from this electrode or dynode are in turn, focussed onto another dynode. The process is repeated for as many stages as is desired. In practice the number of stages is limited by the overall voltage and by the difficulty of electrode design.

The number of secondary electrons, emitted from the dynode, depends on the work function of the surface and the velocity with which the primary beam strikes it.[6] If there are 'n' stages, then the overall current amplification is ideally, $M= m^n$, where m is the gain per stage.

It has been found[7], that for primary electron velocities lying between 20 and 1000 electron volts the great majority of of secondary electrons are emitted from all surfaces with velocities lying between 2 to 6 electron volts. These are regarded as true secondaries. Consequently, the current amplification is dependent not only on the surface but also on the voltage existing between each electrode. Multipliers are usually designed to operate with equal voltages between stages. If then the overall voltage fluctuates, its variations will be reflected in the output current of the tube, so that the supply must be well regulated.

Investigation[7], of the secondary emission ratio 'm' as a function of the primary current up to 5000 electron volts, reveals , in general, that 'm' increases with V_p, passes through a broad maximum lying between 400 and 800 electron volts and slowly decreases as V_p further increases. The highest values of 'm' have been found for composite surfaces such as Mg-Ag (IO at 400 ev) and Cs-Cs_2O-Ag (8 at 400ev) . Unfortunately, these surfaces give off a copious stream of thermionic electrons even at room temperature so that if used as emissive surfaces there is a high current output even when the photocathode is not exposed to light. The noise of this current limits the detection of signals. Consequently, a compromise has to be struck in order to have low thermionic emission allied with good photoelectric and secondary emission.

The surfaces[8] so far found to be suitable are the Sb-Cs and Cs-Bi combinations. The former combines a good spectral response with a low thermionic current. It is useful in the UV to Yellow regions of the spectrum and its threshold occurs at about 6,500 A. The latter surface extends a little further into the red regions of the spectrum, having a threshold at 7,500 A. Its relative spectral response is , however, much poorer than the former.

Because of the difficulty of thermionic emission, no satisfactory multiplier has been developed as yet for the red regions of the spectrum.

Since the photoelectric and secondary emission is instantaneous , the frequency response of the tubes is flat up to those frequencies at which the transit times of the electrons becomes appreciable. The response to light fluxes has been found to be linear over a range of photocathode current of 10^{-20} to 10^{-9} ampere.

Many different types of electrode structure have been designed. The particular tubes used in all this work employ a circular arrangement as shown in figure 4.

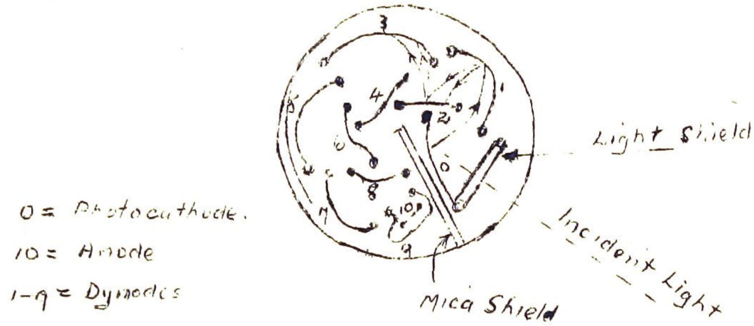

fig. 4

B. The Detection of Small Light Signals

In any measurement of small signals the limit is determined by the magnitude and nature of the fluctuations inherent in the recording equipment. The fluctuations may be either systematic or random in nature and great or small in size. In most circumstances disturbances which are systematic can be overcome with suitable precautions. On the other hand random fluctuations which may be considered to be the aggregate of a large number of elementary disturbances originating from a great number of unrelated sources , cannot be reduced completely to zero.

These inherent disturbances , which vary in an irregular arbitrary manner are technically described as noise. Statistically, they are characterised by no sharply predominant frequency.

Since noise by nature is random, its treatment is statiscal. Again, since no information can be given as regards instantaneous values, conclusions must be expressed in terms of mean values. It is in terms of these mean values that the signal limit in both accuracy and detection is defined.

In the detection of signals with [redacted] a thermionic amplifier, thermal agitation of the electrons in the grid resistor of the first. tube together with the noise from the tube itself, determine the limit. It is here that the signal has its least value, In photometers developed to reveal the presence of small light intensities additional noise arises in the phototube. Furthermore when such photometers are applied to Astronomical observation scintillation is the cause of a further random disturbance. This may be termed atmospheric noise.

When the faintness of the signal is such that it is masked by the noise remaining as the natural limit of the circuit, the only possible remedy is to raise the level of the signal.

Simple phototube photometers have their signal limit defined by the noise level of the following amplifier. The advantage of the photomultiplier is that the virtual limit of the circuit is determined not, by the noise of the following circuits , but by the shot noise of the current between the cathode and the first. dynode.

Since the smallest light fluxes found in practice are those which occur in Astronomy, the advantages of the photomultiplier are best revealed by comparison with a photometer which uses a simple phototube. Such a discussion must be based on the virtual light limit of the two methods together with the delicacy and complexity of the measuring technique.

B (i) Noise in Amplifiers

The most fundamental and inevitable source of noise in an amplifier arises from thermionic noise in the grid resistor of the first tube.Here, the signal is at its lowest. Consequently the aim in amplifier design is to reduce all other sources of noise below that of thermal agitation. These other sources are indigenous to the tube.

The input element of astronomical photometers is a high resistence 'R' in parallel with its own shunt capacity, and that of its leads and of the input of the amplifier. In such circuits the external noise alone is important. This external noise is made up of the grid resistor noise and the shot effect of the grid current.

The mean square noise voltage appearing across the grid resistor due to thermal agitation is[9],

$$\overline{E_r^2} = 4\,k\,T\,R \int_0^\infty \frac{df}{I + 4\pi^2 R^2\, C^2\, f^2} \quad \text{-----(I)}$$

Where

$k = I.37 \times IO^{-I6}$ erg/degree

T = Absolute Temperature

f = frequency in cycles per second

C = the dynamic input capacity of the first tube.

Now, there will be some value of 'f' for which

$$f = f_o = \frac{I}{2\pi RC} \quad \text{---------- (2)}$$

Substitution in (I) and integrating gives

$$\overline{E_r^2} = 2\,\pi\,k\,T\,R\,f_o \quad \text{-------- -(3)}$$

Again, the mean square noise voltage due to the shot effect of the grid current is given by,

$$\overline{E_g^2} = 2eI_g\,R^2 \int_0^\infty \frac{df}{I + 4\pi^2\,R^2\,C^2\,f^2} \quad (4)$$

Where e = the electronic charge $= I.6 \times IO^{-I9}$ coulomb

I_g = the grid current in ampere.

Whence, by considerations similar to those that led to equation 3,

$$\overline{E_g^2} = \pi e I_g R^2 f_o \qquad \text{----------(5)}$$

The total amplifier noise is therefore

$$N = \overline{E_n^2} = \overline{E_r^2} + \overline{E_g^2}$$

Consequently, if S be the signal current , the total signal to noise ratio of the amplifier is

$$\left(\frac{S}{N}\right)^2 = \frac{S^2}{\left(\frac{2\pi kT}{R} + \pi e I_g\right) f_o} \qquad \text{------ (6)}$$

From equation (6) it follows that to increase the signal to noise ratio of such an amplifier

(a) R must be made as large as possible

(b) I_g must be made as small as possible

The optimum resistor will be given by

$$R = \frac{2kT}{eI_g}$$

The signal to noise ratio will be increased by only 40% if R is made infinite.

Special tubes which are characterised by extremely small grid currents (of the order of IO^{-I5} ampere) have been developed. However the input capacity of such tubes cannot be reduced much below $I.6 \times IO^{-II}$ farads so that if R is made greater than IO^{II} ohms the time constants of the circuit become unduly long. Moreover the apparatus becomes complex since the amplifier has to be housed in evacuated and well shielded surroundings.[IO] The measuring technique is delicate[II].

B (ii) Noise from the Phototube

The shot noise from the photoelectric

current is given by,[I2]

$$\overline{I_p^2} = 2\,M^2 e\,I_s\,df \qquad \text{----------(7)}$$

Hence, the mean square noise voltage produced across the grid resistor is

$$\overline{E_p^2} = 2\,M^2\,e\,I_s\,R^2 \int_0^{\infty} \frac{df}{I + 4\pi^2R^2C^2f^2} \qquad \text{--(8)}$$

Consequently,

$$\overline{E_p^2} = \pi e I_s\,R^2M^2f_o \qquad \text{------------(9)}$$

Where I_s is the photoelectric currentand M is the Multiplication within the tube.

B (iii) Seeing Noise from Stellar Scintillation

Astronomical photometry is complicated by stellar scintillation. The classical explanations of this phenomenon [I3,I4,I5], have recently been questioned,[I6,I7,I8], but, observation reveals three distinct effects.

(a) A real and apparently random variation in the intensity of the starlight.

(b) Fluctuations in the position of the star in the focal plane of the eyepiece at right angles to the line of sight.

(c) Fluctuations in the point of focus of the incident rays.

A fourth source of noise may be the random arrival of the light quanta themselves but this is of no importance until surfaces with a quantum efficiency greater than 30 °/o are developed.

The ideal photometer would produce results whose accuracy was limited only by the degree of seeing, of which the chief factor is (a). This variation in the light intensity will be reflected in the photocurrent and hence impressed on the grid of the amplifying tube. The 'b' ,'c' and 'd' effects may also contribute to the noise since there is a tendency for the sensitivity of the cathode to vary over its area. In the case of the Photomultiplier where the sensitivity is rather critically defined[19,20], 'b' and 'c' might be important.

The intensity variations of starlight have been studied[21]. The mean square fluctuations in intensity have been empirically expressed as

$$\overline{\mathcal{J}^2} = \left(\frac{\text{[illegible]}}{D}\right)^{2b} c^2 \mathcal{J}^2 \sec \xi \qquad \text{----(IO)}$$

Where $\mathcal{J}$ = the intensity of the starlight

ξ = zenith distance

D = aperture of the telescope

and c and b are constants.

The frequency of these fluctuations was found to be of the order of hundredths of a second.

Consequently the mean square noise voltage developed across the grid resistor may be written as

$$\overline{E_s^2} = A \sec \xi \; I_s^2 M^2 R^2 f_o \qquad \text{------(II)}$$

A is the seeing constant. This means that although the bright stars yield more noise voltage at the input grid than faint stars, the signal to noise ratio of starlight is independent of the magnitude of the star. It is however, a function of the altitude being greatest for stars in the zenith and least for stars on the horizon.

B(iv) The Amplifier Limit.

The amplifier limit can be defined as that condition for which the amplifier noise is equal to the signal noise.

Ie $\overline{E_r^2} + \overline{E_g^2} = \overline{E_s^2} + \overline{E_p^2}$

whence from equations (3),(5),(9) and (II),

$$M^2 = \frac{2\pi kT}{R[\pi e I_1 + A\sec\zeta\, I_1]^2} + \frac{\pi e I_g}{[\pi e I_1 + A\sec\zeta\, I_1]^2} \quad \text{----(I2)}$$

It follows therefore that for given conditions there is a value of M such that the phototube and seeing determine the limit.

The simple phototube can give rise to an amplification M by gaseous multiplication. However, the multiplication[22] of such tubes is at most I00. Consequently, to develop conditions where the photocell and seeing limit the signal , large input resistors are required with a corresponding increase in the time constant of the circuit.

B(v) Noise in Electron Multipliers

The complete theory of noise for electron multipliers was given in 1938.[23] The final expression for the mean square noise current associated with an 'n' stage multiplier was found to be

$$\overline{I_n^2} = M^2\,\overline{I_p^2} + 2e\,\overline{I_n}\,M\left[b_1 + \frac{b_2}{m_1} + \cdots\cdots \frac{b_n}{m_1 m_2 \cdots m_{n-1}}\right]\Delta f \quad \text{----(I3)}$$

Where $\overline{I_n^2}$ = the noise current in the output stage.

I_n = the direct component of the input current.

m_r = is the amplification of the rth stage

$\overline{I_p^2}$ = the mean square shot noise in the input

$b_r = \frac{\delta_r^2}{m_r}$ = relative mean square deviation of m_r.

δ_r^2 = mean square deviation of m_r.

$M = (m_1 \times m_2 \cdots\cdots m_n)$ = the overall multiplication

It can be seen from (I3) that the first term is merely the shot noise in the first stage of the tube. In the derivation no assumption is made as to the nature of this noise.

When a single stage only is considered the result becomes,

$$\overline{I_f^2} = m^2 \overline{I_p^2} + 2e\overline{I_s}\, mb\,\Delta f \qquad \text{-----(I4)}$$

This equation indicates that each stage introduces a noise proportional to

(a) the average current leaving the stage

(b) the product 'mb' of that stage.

The genesis of each component of the second term follows immediately.

If the rth factor is considered

$$2e\overline{I_n}\, M \frac{b_r}{m_1 m_2 \cdots m_{r-1}}\,\Delta f$$

Which can be written as,

$$[2e\overline{I_1}\, m_1 m_2 \cdots m_r \Delta f][m_r b_r][m_{r+1} \cdots m_n]^2$$

and may be represented by, AxBxC. Then A is just the expression for the shot noise corresponding to the output from the rth plate; B is the modifying factor 'mb' for the stage; C is the multiplication for all the subsequent stages.

If 'm' and 'b' are the same for all stages (I3) may be summed to give,

$$\overline{I_n^2} = M^2 \overline{I_p^2} + 2e\overline{I_n} \times \left(\frac{M-1}{m-1}\right) mb\,\Delta f \qquad \text{----(I5)}$$

Therefore for a given 'm' the most important quantity is 'b'. If 'b' is zero, the multiplier itself introduces no noise but amplifies only that present in the input.

Equation (I5) may also be written as

$$\overline{I_n^2} = M^2\overline{I_p^2} + 2e\bar{I}_p M\left(\frac{M-1}{m-1}\right) mb\, df \qquad \text{-------(I6)}$$

In their original paper Zworikin, Malter and Morton developed a noise theory based on the assumption that the number of secondaries emitted per primary could be any value from zero to N. The probability that an electron be emitted is m/N. If m is held constant while N is allowed to go to infinity the Poisson distribution is obtained.

viz.
$$p(g) = \frac{m^g e^{-m}}{g!}$$

Where p(g) is the probability that 'g' electrons are emitted.

From the properties of the [illegible] distribution it follows that $b = (m)^{-I}$. For all practical purposes the Poisson distribution may be assumed. Consequently, if the shot noise in the input current is

$$\overline{I_p^2} = 2e\bar{I}_p df \qquad \text{-----(I7)}$$

then, (I6) becomes,

$$\overline{I_n^2} = 2e\bar{I}_p M\frac{(Mm-1)}{m-1} df \qquad \text{-----(I8)}$$

Under ordinary circumstances $Mm >> I$, so that in practice calculation of the noise current in the output of the photomultiplier can be based on

$$\overline{I_n^2} = \frac{m}{m-1} 2e M^2 I_p df \qquad \text{-----(I9)}$$

It is evident from (I9) that for m= 5 , [illegible]5% of the noise is due to statistical [illegible] fluctuations in gain. In one application this variation in gain has been found to set the limit to the accuracy of measurement.[a]

---

[a] Private communication from Dr. Giovanelli, Photometry Division of the CSIRO, Sydney, N.S.W.

B(vi) Comparison of the Photomultiplier with a simple Phototube

From considerations similar to those which led to equation (I2), the amplifier limit when a simple photocell is replaced by a photomultiplier can be found. For the same conditions then,

$$M^2 = \frac{2\pi kT}{R\left[\frac{m}{m-1}\pi e I_p + \pi I_p^2 \sec\xi\right]} + \frac{\pi e I_g}{\left[\frac{m}{m-1}\pi e I_p + \pi I_p^2 \sec\xi\right]} \quad \text{-----(20)}$$

A practical value for m is m=5. Using this value (20) becomes,

$$M \geq 10^{-10}\sqrt{\frac{2.60}{\left[6.3\times10^{-19}I_p + AI_p^2\sec\xi\right]R} + \frac{50 I_g}{\left[6.3\times10^{-19}I_p + AI_p^2\sec\xi\right]}} \quad \text{-----(2I)}$$

Case I $AI_p^2 \sec\xi = 0$

This case may be taken as representing conditions in which the photometer is used for measuring steady light sources. As mentioned in section A and is discussed in section C there is a measurable output due to thermionic current even at room temperatures. It is of the order of 10^{-13} ampere and in the following discussion this value will be assumed.

Consequently, equation (2I) becomes,

$$M \geq 2\times10^{6}\sqrt{\frac{1}{R} + 20 I_g} \quad \text{-----(22)}$$

Similar reasoning applied to (I2) gives a value slightly greater than (22) since they differ only by m/(m-I).

In practice , therefore, equation (22) will give the order of multiplication reuired to set the amplifier limit in both cases.

The general type of amplifier tube has a grid current of the order of 10^{-9} ampere so that for a following amplifier designed about these tubes

$$M_A \geq 2\times10^{6}\sqrt{2\times10^{8} + \frac{1}{R}} \quad \text{---- (22.I)}$$

On the other hand, an amplifer employing electrometer tubes would have an amplifier limit defined by

$$M_E \geqslant 2\times10^6 \sqrt{2\times10^{-14} + \frac{1}{R}} \qquad \text{------(22.2)}$$

These equations indicate that the minimum multiplication is given approximately by

$$M_H \doteqdot 2\times10^6 R^{-\frac{1}{2}} \qquad R < 10^6 \Omega$$

$$M_E \doteqdot 2\times10^6 R^{-\frac{1}{2}} \qquad R < 10^{12} \Omega$$

It can be seen that when M becomes such that ordinary gas multiplication can be used the time constants of the circuit begin to become long. It is also to be noticed that the minimum amplification able to be used with ordinary amplifier tubes is of the order of 300 which is much too large for gas multiplication.

Case II $A \sec \xi \neq 0$

If $\sec \xi$ = I the equation gives the necessary value for M for either

(a) Photometry of Zenith stars

or

(b) The direct recording of spectral line intensities from , say, an arc source. A in this case would describe the noise associated with the sputtering of the arc. A , in general, describes the random fluctuations of the source.

C(i) The Dark Current

The dark current may be ascribed to ... three causes[24],

(a) Ohmic Leakage

(b) Thermionic Emission

(c) Regenerative Ionisation

Ohmic leakage arises from leakage over the deposited Cs , on the walls, and from leakge over the base and the socket. As can be seen from figure 5

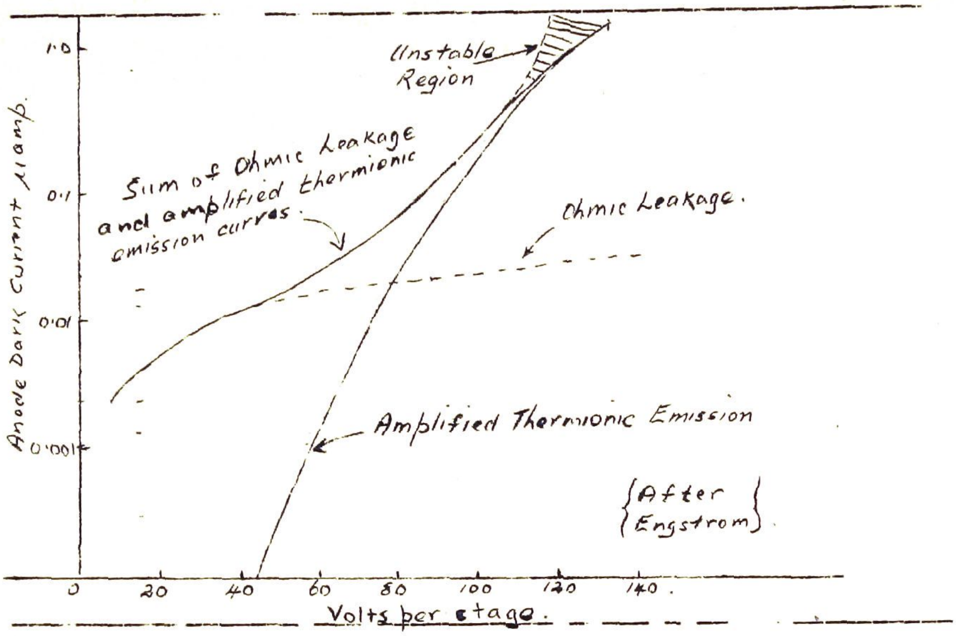

Figure 5

this leakage is the dominant factor up to about 60 volts per stage. If this is subject to random and sudden fluctuations it can be disturbing. The more recent tubes[25] have a separate anode cap in order to increase the leakage paths between the anode and the dynodes. We have found by removing the anode lug from the socket and connecting directly to the anode pin that the dark current is reduced by a factor of IO. Removal of the anode pin altogether has been advised.[26]

Above 60 volts per stage the dark current due to thermionic emission becomes important. It increases with increase of voltage per stage , as is to be expected since it is amplified in the same manner as a signal.

For voltages per stage greater than IIO volts instability begins. This is due to positive ion feedback and is a regenerative ionisation process. The tube tends to break down between I40 and I80 volts per stage.

Because of this instability it is customary to operate these tubes between 60 and 110 volts per stage depending on the current gain required.

C(ii) Techniques for the reduction of Dark Current

Provided equation (20) is satisfied the noise of the photometer may be described by equation (19). Consequently, the remedy for increasing the signal to noise ratio when the signal is such that it is equal to the noise, is

(a) Increase the signal

(b) Reduce the noise

In the regions where the thermionic current is dominant the logical approach to reducing I_t are

(i) Reduce the cathode area

(ii) Increase the quantum efficiency

(iii) Reduce the temperature

To the user (iii) is the only practical method.

A close study of the effects of temperature reduction has been made by Engstrom. A temperature variation from +40°C to -190°C revealed an increase in the signal to noise ratio of the order of 40 decibel. The estimated limit was 2×10^{-16} ampere ; the equivelent of a photocathode current of 2×10^{-21} ampere. A very small light flux indeed.

Such small currents require special techniques which, though complicated, are not as delicate as electrometer or electrometer tube amplifier methods. When a Photomultiplier tube is operating with a gain of 10^5 it means that for every electron leaving the cathode , on the average the above number reach the anode. This generation may be compared to the Geiger counter mechanism and the counting circuits developed for use with them may be equally as well applied to the burst of electrons from the Photomultiplier tube. It becomes possible to count the individual electon pulses. The only requirement is that they be counted for long enough to be statistically sure of the number of electrons per unit time. Moreover if the pulses are observed on a Cathode Ray Oscillograph, the distribution of pulse heights will be found to be skew, with the majority of the pulses small. Such small pulses will necessarily be due to electrons emitted from the various secondary stages within the tube and their height will be dependent on the overall multiplication they have undergone. If it is arranged to discriminate against these smaller pulses the signal to noise ratio may be further increased.

C(iii) Coincidence Counting Techniques ?,27,28

Electron Multiplier tubes have been found to posses distinct advantages in the field of particle counting. Their ability to detect small light fluxes has given rise to the use as scintillation counters. The noise problem has been quite ingeniously overcome. Two or three multipliers are arranged so as to look at the various faces of the crystal. The output of the multiplier is fed into a double or triple coincidence circuit.

Since the thermionic emissive process is entirely random, the chances of coincidences are small. However, when a particle strikes the crystal the cathodes of the tubes are simultaneously energised giving rise to a coincidence count. In this manner the noise level can be reduced to one or two counts per five minute interval.

D. Conclusion.

The characteristics of the Photomultiplier have been outlined in order to demonstrate its usefullness in the detection of weak light sources.

However, while it is eminently suitable for weak sources it ceases to possess any advantage over the simple photocells when the light intensities are large. Furthermore, in the red regions of the spectrum a simple type cell must be used.

The limitations of signals by noise has been treated in some detail because noise has played an important part in the attempt to develop a photoelectric recorder of stellar transits. Moreover, the various difficulties attendent to the detection of weak light sources by ordinary photometric means has been mentioned in order to indicate the advantages accrueing from a successful method of recording intensity distributions and the automatic counting of fringe shifts.

Chapter III

The Intensity Distribution of Fringe Systems and the Automatic Counting of Fringes.

A) Introduction

It is customary to consider interference under two headings. When the interference effects can be considered to be due to the superposition of individual wavelets of the wave front the resultant redistribution of the light is termed diffraction. On the other hand, when the superposition arises from the combination of two or more beams that have originally issued from from the same source, the redistribution of the light is called interference. Instruments which perform the separation and recombination are called interferometers.

The patterns that arise in interferometers can be due to a redistribution of the light or a complementary pattern is formed elsewhere. In the first case the brighter parts collect energy from the darker portions. Although the brighter portions of the pattern are more intense than would be expected from the addition of two beams of equal intensity, the mean intensity of the pattern is equal to the sum of the two separate intensities. Fresnel's Biprism, the Diffraction Grating and the Lummer Plate are examples of this class. However, with Newtons Rings and the Michelson and Fabry-Perot interferometers complementary patterns are formed. The bright portions of the complementary pattern correspond to the dark portions of the observed pattern.

Interferometric techniques are developed about two essential principles,

(a) Division of Wavefront

(b) Division of Amplitude

With the first class the greater the area over which the wavefront must be in phase, the smaller must be the angle the source subtends at the wavefront. Methods based on this principle require a point or line source. If the point or line source be greater than a certain optimum value the fringes disappear. The coherent wavefronts, emerging in slightly different directions from the source are further separated by mirrors, prisms or lenses and finally brought together to form the interference bands. The Fresnel Biprism and Bimirror, the Trimirror system of Vautier[29], the Billet split lens and the Rayleigh Refractometer belong to this class.

The second principle is applied by dividing the beam by partial reflexion at a silvered mirror. The transmitted and reflected beams retain a point to point correspondence so that any peculiarities in one are also present in the other. Consequently, however complex the original wavefront is, the clearness of the interference effects is not impaired. In general, therefore the effects are much brighter since it allows an extended source to be used. The interference patterns of thin films, the interferometers of Jamin, Mach-Zehnder, Michelson and Fabry-Perot rely on this principle.

In special instances, interferometers in the second category can be modified and used as an instrument of the former class. There is both a division of wave front and amplitude. It has many additional qualitied and behaves in an entirely different way. The classical examples are the Twyman and Green modification of the Michelson and the Fizeau interferometer. The interferometer developed in the course of this work and described in a later section is another instance of the combination of the two principles.

B) The Fundamentals of Interference Optics

(i) Interference

In the consideration of interferometers as described in section A, the wave nature of light is taken into account in so far as several coherent pencils are combined, this being done in such a way as to allow for their difference in phase. The diffraction phenomena occuring at the boundaries are not of essential importance in this type of device.

When a plane wave is reflected from a wedge of small angle the superposition of the waves reflected from the back and front sides of the wedge will yield an increased or decreased resultant disturbance depending on the phase difference of the emerging waves. This phase difference depends only on the optical path between the two faces of the wedge. Consequently, there will be places where the disturbance is intensified and others where it is weakened. The resulting illumination depends on whether the path difference at the front surf-- is an integralnumber of whole wavelengths or half wavelengths. In the former instance, the resulting illumination is intensified, in the latter instance it is weakened. The eye or photographic objective focussed on the upper surface of the wedge will see a system of light and dark bands. These are the equi-thickness curves of the wedge. If the angle of the wedge is not small, the rays at a given point have different path differences. The visibility of the fringes decreases considerably even for monochromatic light . Also, if the divergence of the incident beam is too large so that the path difference at a given point of the wedge is not the same for all rays , the visibility of the fringes will be impaired.

Conversely, if a divergent beam is allowed to fall on a plane parallel plate, the difference in inclination of the rays gives rise to a path difference between the rays reflected from the two surfaces. This path differnce is $2t\cos\alpha$.

Where t= thickness of the plate

α = angle of incidence

and the index of refraction of the plate is the same as that of the surrounding medium.

For those directions where

$$2t \cos \alpha = p\lambda \quad \text{(with p integral)} \quad \text{---(i)}$$

there is light. But, for those directions where

$$2t\cos \alpha = (p+\frac{1}{2}) \lambda \quad \text{-----(ii)}$$

there is darkness.

Since there is complete symmetry about the normal, all rays making an angle 'α' with the normal yield a circle in the focal plane of a telescope focussed for infinity. The fringe system therefore consists of concentric circles.

Again, if the superposition of the two coherent waves is brought about by diffraction as in the case of Fresnel or Fraunhoffer diffraction through a double slit the same conditions (i) and (ii) apply. The fringes are no longer localised at a surface of at infinity however, but may be considered to be localised in space.

Nevertheless, it was precisely this diffraction effect being used to produce interference that gave rise to adverse criticism of Young's experiments. The independent developement of the wave theory of light by Fresnel was climaxed by his bimirror and biprism demonstrations of interference. By such methods interference occurred without the aid of diffraction to bring the beams together.

Unfortunately, all such classical methods give patterns which are complicated by a subsidiary diffraction envelope. This diffraction arises from the fact that the waves proceeding from the virtual sources are abruptly cut-off at some point of union in the apparatus. Besides complicating the pattern it sets a limit to the accuracy with which the centre of a fringe can be judged. It was precisely this modulation by diffraction that presented the chief difficulty to the attempt to count fringe shifts photoelectrically.

(ii) Diffraction

The disturbance at a point P situated on the opposite side of a plane screen to a source Q, when the screen contains an aperture is given by, (Joos: Theoretical Physics p367)

$$u_p = \frac{i\{\cos(\check{n}\check{r}) - \cos(\check{n}\check{r}_q)\}}{2\lambda R R_q} e^{-ik(R+R_q)} \int_{\text{Wave front}} e^{-ik\phi(\xi,\eta)} dS \quad \text{---(I)}$$

Where $\check{\eta}$ = unit normal to the plane of the screen

$\check{r}_q$ = radius vector drawn from Q to a point of the aperture

$\check{r}$ = radius vector drawn from the point to the same point of the aperture

R_q = distance of the point source from the origin of the co-ordinates

R = the distance of the observer from the origin

$k = 2\pi/\lambda$

dS = element of area of the wave front.

and

$$\phi(\xi,\eta) = \xi(\alpha_0-\alpha) + \eta(\beta_0-\beta) + \frac{1}{2}\frac{\xi^2+\eta^2}{R_q} + \frac{1}{2}\frac{\xi^2+\eta^2}{R} - \frac{1}{2}\frac{(\alpha_0\xi+\beta_0\eta)^2}{R_q} - \frac{1}{2}\frac{(\alpha\xi+\beta\eta)^2}{R} \quad \text{----(2)}$$

where ξ, η are the co-ordinates of the point of the aperture

α_0, β_0 = direction cosines of the line R_q

α, β = direction cosines of the line R

If the points P and Q are situated at distances such that the terms containing ξ and η to the second degree are small, then substitution of $\phi(\xi,\eta)$.

in equation (I) will express Fraunhoffer Diffraction phenomena. On the other hand, if conditions are such that the second order terms cannot be neglected then equation (I) containing the appropriate expression for $\phi(\xi,\eta)$ will describe Fresnel Diffraction effects.

<u>(a) Fraunhöffer Diffraction by N slits.</u>

In this case $\phi(\xi,\eta)$ reduces to

$$\phi(\xi,\eta) = \xi(\alpha_0-\alpha) + \eta(\beta_0-\beta).$$

Let the width of the slits be 'a' and length 'b' such that 'b' >> 'a'. Moreover, if 'i' and 'θ' are the angles the incident and diffracted rays make with the slit then,

$$\phi(\xi,\eta) = \xi(\sin i - \sin\theta)$$

If the distance between the centres of the slits be 'd' a d the opaque potion be of width 'c' then,

$$U_p = Const \sum_{M=0}^{(N-1)} \int_{Md-\frac{a}{2}}^{Md+\frac{a}{2}} e^{-i\mu\xi}\, d\xi. \qquad \text{----(I.}$$

where the origin of the system is taken as the centre of the first slit and

$$\mu = 2\pi(\sin i - \sin\theta)/\lambda \qquad \text{----(I.}$$

Integration gives

$$U_p = Const \frac{\sin\beta}{\beta} \sum_{M=0}^{N-1} e^{-iM\mu d}$$

where $\beta = \pi(\sin i - \sin\theta)a/\lambda$

Now, $\sum_{M=0}^{N-1} e^{-iM\mu d}$ is a geometrical progression summed to N terms

ie $$U_p = U_0 \frac{\sin\beta}{\beta} \frac{\sin N\gamma}{\sin\gamma} e^{-i\phi}$$

where $\phi = \frac{N-1}{2}\mu d$

Whence ,

$$I = I_0 \frac{\sin^2\beta}{\beta^2} \frac{\sin^2 N\gamma}{\sin^2\gamma} \qquad \text{-----} \quad (I\cdot iii).$$

Case of N = 2

Equation (I.iii) reduces to

$$I = 4 I_0 \cos^2\gamma \, \frac{\sin^2\beta}{\beta^2} \qquad \text{----(I.iv)}$$

ie $$I = I_f \times I_D$$

Where $I_f = 4\ I_o \cos^2\gamma$ is the intensity distribution corresponding to the wavefronts proceeding from two coherent sources. On the other hand I_d is the modulation of this primary pattern owing to wavefronts being distorted in shape by the edges of the slits. The resultant intensity distribution is a function of both γ and β. They are not independent.

The expression for I_f is characteristic of interference patterns produced by two coherent beams of equal intensity and whose phase difference is $\delta = 2\gamma$. This is the distribution graphed in chapter I in which the pattern is assumed free of any diffraction whatsoever.

(b) Fresnel Diffraction and the Cornu Spiral

Suppose the source to be a line of light of infinite extent in the η. direction and that the normal from the point of observation to the line source passes through the edge of a slit and is perpendicular to the plane of the screen.

In this case $\alpha_o = \alpha = 0$ and

$$\phi(\xi, \eta) = \frac{\xi^2}{2}\left\{\frac{1}{R} + \frac{1}{R_q}\right\}. \qquad \text{(I.v)}$$

Whence,

$$u_p = \text{Const} \int_0^{\xi} e^{-\frac{i\pi}{\lambda}\left\{\frac{1}{R} + \frac{1}{R_q}\right\}\xi^2} d\xi$$

Let

$$v = \xi\sqrt{\frac{2}{\lambda}\left(\frac{1}{R} + \frac{1}{R_q}\right)}.$$

Then,

$$U_p = Const \int_0^v e^{-\frac{i\pi}{2}v^2} dv \qquad \text{-----(I.vi)}$$

The curve $z = \int_0^v e^{-\frac{i\pi}{2}v^2} dv$, whose parametric equations in rectangular coordinates are

$$x = \int_0^v \cos \frac{\pi}{2} v^2 dv \quad \text{and} \quad y = \int_0^v \sin \frac{\pi}{2} v^2 dv$$

is called the Cornu Spiral.

The integrals themselves, give upon integration infinite series[30] which may be evaluated in several ways. Tables of these Fresnel integrals for values of the argument 'v' from 0 to 5 can be found in most textbooks on optics.[31] However, values for arguments greater than 5 appear to have been done only once.[32] They are for v=5 to v=8.5.

Once the spiral has been drawn it can be employed to answer a number of questions approximately. For specific problems the tabulated values may be used. Although tedious the method is most accurate.

C. The Intensity Distribution of the Fresnel Biprism

For various reasons but chiefly its simplicity the particular method of producing interference fringes, chosen initially, was the Fresnel Biprism. The fringes are easy to find. The apparatus is simple. The counting of the fringes produced by it might have advantages in applied optics.

In order to gain some idea of the light distribution several sweeps of the pattern were made. (Figures 6,7 and 8). To select the fringes a second slit of adjustable width was placed at some convenient point along the optical bench. With the patterns of figures 6 and 7 a low power microscope was focussed on the slit. The photomultiplier looked at the eyepiece of the microscope in precisely the same manner as the arrangement for the telescope.(See section D Chapter III).

Since the microscope method cut down considerably on the available light the technique was changed for plot 8. In this case the selecting slit was placed some 300 cms from the biprism and a Ramsden eyepiece focussed on the slit which had been adjusted to a fraction of the width of a fringe. A length of pipe extending from the biprism to the selecting slit cut down on the amount of stray light entering the system.

The fringes were swept passed the selecting slit by mounting the biprism on on a fine screw travel. The output of the Photomultiplier was amplified by a bridge type amplifier in the case of plots 6 and 7 and figure 6 is of interest because it indicated that a successful method must employ a highly stable amplifier. The high rate of drift evidenced in plot 6 would never do.

Figure 7 is a later plot in which the instability of the amplifier was somewhat overcome by rebalancing the amplifier at zero light before each and every reading of the milliameter. Figure 8 is a later plot in which the amplifier of figure 9 was used. Its stability was such that direct runs could be made across the pattern.

It was evident, from figures 7 and 8 which, in their essential characteristics, are identical that the modulation of the system by the diffraction pattern would make the presetting of a trigger circuit impossible. This enveloping pattern caused some minima to be greater than some maxima in absolute intensity. In any fringe sweep therfore, some fringes would most certainly be missed.

In order to check these distributions the biprism patterns were photographed and the intensity variations recorded with a Moll micro-photometer. Fig IO is a print of the pattern in which diffraction almost masks the interference. Fig II is a print and fig. I2 a microphotometer trace with constants similar to those plotted with the Photomultiplier tube.

Examination of these patterns reveals

(i) When the width of the diffraction bands is large there are variations in the absolute intensity of the maxima and minima of interference with some minima greater than some maxima.

(ii) At the centre of the pattern where the width of the diffraction bands becomes of the same order as the interference fringes there is an alternation in the intensity of the interferencemaxima.

(iii) The pattern is asymmetric ; the first diffraction maxima of one side being greater than the first maxima of the other.

D. Theory of the Fresnel Biprism Pattern

The diffraction pattern is due to the straight edge presented to the incident wave by the vertex of the biprism. If the system be considered from the point of view of the two virtual sources then the vertex B (figI3) of the prism ABC presents a straight edge to the virtual source S'. Similarly, vertex B of the prism ABD is a straight edge with respect to the virtual source S''.

A straight edge diffraction pattern will arise therefore at the geometrical shadow of S' with respect to B, and a corresponding pattern will arise at the geometrical shadow of S'' with respect to B. The extent with which these influence the

$\cos^2\gamma$ distribution will depend on the constants of the experimental arrangement. If they are such that the effect of the diffraction pattern is small , then, at the centre of the pattern a true $\cos^2\gamma$ distribution will be observed.

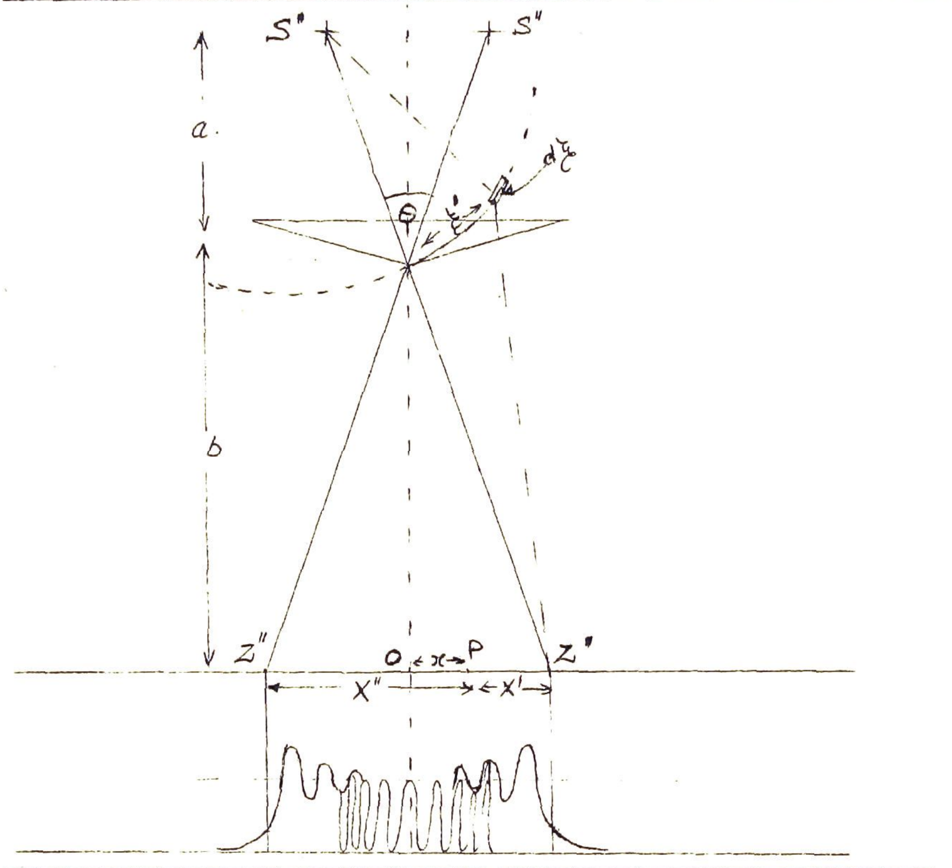

Figure I3

The complete distribution can be considered to be the superposition of wavefronts deformed by diffraction. The resultant amplitude at the point P (fig. I3) will be that arising from the sum of the displacements of the two waves at this point with due regard to phase.

Introducing the time factor into equation (I) , the displacement at P due to the wave proceeding from the line source S' is

$$u'_p = \frac{i\{\cos(n''\xi) - \cos n''\xi_q\}}{2\lambda ab}\, e^{i2\pi(\nu t - \frac{D}{\lambda})} \int_0^{\xi'} e^{-ik\phi(\xi)}\, d\xi \quad \text{---(I.a)}$$

in which it is assumed that $\alpha = \alpha_0 = 0$.

Since the wave front is symmetrical, the integration may be performed over an element of the wavefront $d\xi$. (fig I3). Also, if the enquiry be limited to points not too far from the geometrical shadow, the obliquity factor [33] and the decrease of amplitude with distance may be neglected. For large distances from the geometrical shadow, the following treatment will represent the conditions approximately. Resorting to real quantities equation (I.a) becomes,

$$u'_p = A'\cos 2\pi\left(\nu t - \frac{D}{\lambda}\right)\int_0^{\xi'} \sin\frac{2\pi}{\lambda}\phi(\xi)\,d\xi - A'\sin 2\pi\left(\nu t - \frac{D}{\lambda}\right)\int_0^{\xi'}\cos\frac{2\pi}{\lambda}\phi(\xi)\,d\xi.$$

Where A' = the amplitude of the incident wavefront

$D = (a+b)$

Similarly the displacement due to the source S'' will be

$$u''_p = \left\{A''\cos 2\pi\left[\nu t - \frac{D}{\lambda} - \left(\frac{S'P - S''P}{\lambda}\right)\right]\int_0^{\xi''}\sin\frac{2\pi}{\lambda}\phi(\xi)\,d\xi\right\}$$

$$-\left\{A''\sin 2\pi\left[\nu t - \frac{D}{\lambda} - \frac{(S'P - S''P)}{\lambda}\right]\right\}\int_0^{\xi''}\cos\frac{2\pi}{\lambda}\phi(\xi)\,d\xi.$$

The resultant amplitude at P is therfore,

$$u_p = u'_p + u''_p$$

Assuming for simplicity that the amplitudes are equal and letting,

$$\phi = 2\pi\left(\nu t - \frac{D}{\lambda}\right)$$

$$\delta = \frac{2\pi}{\lambda}(S'P - S''P)$$

$$x = \int_0^{\xi'}\cos\frac{2\pi}{\lambda}\phi(\xi)\,d\xi$$

$$y = \int_0^{\xi'}\sin\frac{2\pi}{\lambda}\phi(\xi)\,d\xi$$

$$X = \int_0^{\xi''}\cos\frac{2\pi}{\lambda}\phi(\xi)\,d\xi$$

$$Y = \int_0^{\xi''}\sin\frac{2\pi}{\lambda}\phi(\xi)\,d\xi.$$

Then,

$$u_p = U_p \cos 2\pi\left(\nu t - \frac{D}{\lambda} + \frac{\theta}{2\pi}\right) \quad \text{---- I.b}$$

where

$$\tan\theta = \frac{x + X\cos\delta - y\sin\delta}{y + Y\cos\delta + X\sin\delta} \quad \text{---- I.c}$$

and ,

$$U^2 = A^2\left\{x^2+y^2+X^2+Y^2+2(yY+xX)\cos\delta-2(xY-yX)\sin\delta\right\} \quad \text{(I.d)}$$

Equation I.b represents a vibration having the same period as the original wave but a different amplitude and phase constant. The phase constant is of little interest but U^2 gives the intensity. Since $\alpha = \alpha_0 = 0$,

$$\phi(\xi) = \xi^2\left(\frac{a+b}{2ab}\right) = \xi^2\left(\frac{D}{a+b}\right)$$

Transposing to a new variable 'v' as in section (B.b) equation (I.d) becomes,

$$U^2 = \frac{A^2ab\lambda}{2D}\left\{(m^2+n^2)+M^2+N^2+2(mM+nN)\cos\delta-2(mN-nM)\sin\delta\right\} \quad \text{(I.e)}$$

Where,

$$m = \int_0^{v'} \cos\frac{\pi}{2}v^2dv \qquad M = \int_0^{v''} \cos\frac{\pi}{2}v^2dv$$

$$n = \int_0^{v'} \sin\frac{\pi}{2}v^2dv \qquad N = \int_0^{v''} \sin\frac{\pi}{2}v^2dv.$$

In particular problems it is better to consider distances X' and X'' on the viewing screen, where X'=0 at the geometrical shadow of S' with respect to B and, X''=0 at the geometrical shadow of S'' with respect to B.

From Figure I3, $\frac{\xi'}{a} = \frac{X'}{D}$; $\frac{\xi''}{a} = \frac{X''}{D}$.

so that,

$$X' = v'\sqrt{\frac{b\lambda D}{2a}} \; ; \quad X'' = v''\sqrt{\frac{b\lambda D}{2a}}.$$

The natural origin of the system is at O , the position of the zero order interference fringe. Since $\frac{b\theta}{2} = b(\mu-1)A$, where A is the angle of the biprism and μ is the refractive index, and since

$$OZ' = OZ'' = \frac{b\theta}{2}$$

v' becomes,

$$v' = \sqrt{\frac{2a}{b\lambda D}}\left\{b(\mu-1)A - x\right\}. \quad \text{---(I.f)}$$

But distances 'x' from the origin

O are given by,

$$n\lambda = \frac{2a(\mu-1)A}{D}x.$$

where 'n' is allowed to take any real value positive or negative.

Therefore equation I.f may be written as

$$v' = \sqrt{\frac{\lambda D}{2ab(\mu-1)^2A^2}}\left\{\frac{2ab(\mu-1)^2A^2}{\lambda D} - n\right\}. \quad \text{---(I.g)}$$

Similarly,

$$v'' = \sqrt{\frac{\lambda D}{2ab(\mu-1)^2A^2}}\left\{\frac{2ab(\mu-1)^2A^2}{\lambda D} + n\right\}. \quad \text{----(I.g)}$$

Now, when 'n' is integral

$$I_{max} = \frac{A^2ab\lambda}{2D}\left\{m^2+n^2+M^2+N^2+2(mM+nN)\cos\delta\right\} \quad \text{----(I.h)}$$

is the condition for a bright interference fringe, while if n be half integral,

$$I_{min} = \frac{A^2ab\lambda}{2D}\left\{m^2+n^2+M^2+N^2-2(mN-nM)\sin\delta\right\}. \quad \text{---(I.k)}$$

is the condition for a dark fringe.

Moreover, when 'n' is zero, I, is given by (I.h) and since v' = v'', m=M and n=N so

$$I = \frac{2A^2ab\lambda}{2D}\left\{m^2+n^2\right\}\left\{1+\cos\delta\right\}$$

$$= \frac{ab\lambda}{2D}\left\{m^2+n^2\right\} \times 4A^2\cos^2\delta$$

$$= I_D \times I_f. \quad \text{-----(I.}$$

Equation (I.l) corresponds to equation (I.iv) of section (B.a)

Again, v' and v'' are zero when 'n' as given by

$$n = \frac{2ab(\mu-1)^2A^2}{\lambda D} \quad \text{----(I.m)}$$

is positive or negative respectively, so that the geometrical shadow is defined by (I.m). Also,

$$I = \frac{A^2ab\lambda}{2D}\left\{M^2+N^2\right\}.$$

With the aid of equations (I.e) and (I.g) and the use of tabulated values of the Fresnel integrals, the expected pattern for a given set of experimental constants can be plotted. It is sufficient to work with integral and half integral values of 'n'.

The best procedure to follow is to determine v' and v'' from (I.g) for particular values of 'n'. Since $\frac{A^2ab\lambda}{2D}$ is constant, values of $\frac{2D}{A^2ab\lambda} I$ may be determined from (I.h) and I.k depending upon whether 'n' is integral or half integral, and the values obtained plotted against 'n'. Figure I4 is such a plot in which the experimental values of figure 8 were used.

Its general characteristics are in harmony with figure 8. An asymmetrical plot in which the different intensities of the sources S' and S'' was taken into account was not attempted.

This asymmetry appears to arise in the Biprism itself, for it seemed to be independent of the alignement of the subsidiary components. Since it was considered to be a minor point a systematic attempt at determining its origin was not carried out.

E. Fresnel Fringes with a Michelson Interferometer

These intensity plots made it evident that if an automatic recording apparatus for fringe shifts was to be developed, some means of producing Fresnel fringes , free from diffraction must be used. The only method satisfying this condition appears to be a demonstration experiment of Michelson[34], in which two mirrors at right angles and a slit source at a very large distance is used. However, the standard three mirror system of Michelson can be adjusted to give a pure $\cos^2 \gamma$ distribution.

The fully silvered mirrors M_1 and M_2 (figure I5) are adjusted for white light fringes using an extended source. This condition implies that the optical and linear paths to the mirrors are exactly equal. If the broad source is replaced by an illuminated slit and one or both of the fully silvered mirrors slightly turned about an axis perpendicular to the plane of the apparatus and parallel to the plane of the slit, two images of the slit are formed. Fresnel fringes may then be observed by looking at the images with a simple ocular.

The best fringe visibility is dependent on the images being parallel and vertical. This is most easily ensured by throwing white light onto the system and adjusting the tilt of the mirrors until the white localised fringes are vertical with the central black fringe in the centre of the fully silvered mirror.

The apparatus becomes a virtual Fresnel bimirror. No diffraction occurs since the point of union in the system is itself virtual. If A be the distance of the slit from 'M' and B the distance of the eyepiece from M' and θ the angle between the mirrors then,

$$\lambda = \frac{2A\theta}{A+B}x.$$

Where 'x' is the width of a fringe.

Figures I6, I7 and I8 are prints of interference patterns produced by this method. In fig. I6 the fringes are quite broad while in fig. I8 they are quite narrow. Figures I9, 20 and 2I are microphotometer traces of typical patterns . While the intensity tends to fall off for fringes of large order , diffraction is absent. Although the method involves both a division of wave front and amplitude the fringes fall neither into the Twyman and Green nor the Fizeau class. They are a pure $\cos^2\gamma$ type with the dark and bright fringes of equal width, and approach the ideal of figure I , chapter I.

F. The Guest Interferometer

A consideration of FigureI5 will reveal that if the fully silvered mirrors are caused to rotate on a circular arc the centre of which is at the half silvered edge of the bisecting mirror , then, the image of M_2 namely M_2' rotates in the opposite sense to M_1. If, initially, the mirrors M_1 and M_2 are at right angles , M_1 and M_2' rotate about an axis which remains on the optic axis of the apparatus. Therefore the slit images remain symmetrically disposed about the optic axis and hence, the fringe of zero order remains central.

Since it was felt desirable to be able to mount the interferometer on an optical bench, the design was carried out with this in mind. Figure22 is a photograph of the interferometer mounted on an optical bench.

The supporting pillar carries a circular plate, IO cms in diameter. In a circular way of 8 cms in diameter on this plate ball bearings are set. An additional circular plate which carries the fully silvered mirrors rides on these balls, about the pillar as axis. On the top surface of this turntable are further balls in a ring 5cms in diameter. A rectangular block to which the half silvered plate and the compensator are fixed presses on these balls and is locked to the pillar. The half silvered mirror can be adjusted so that the axis of the turntable passes through the silvered edge. To facilitate adjustment for white light localised fringes one of the fully silvered mirrors is mounted on ways. It can be moved some two cms about the zero position. Rotation of the turntable is effected by means of a tangent screw. With it, any desired fringe separation can be attained.

The mirrors must be optically flat. In the developemental model the mirrors used were made from not very flat optical glass. With these, it was found that adjustments for high contrast between the light and dark fringes were very critical and unique for a given fringe width. The visibility could not be maintained for all angles.

Now for a constant λ and fringe width,

$$d\theta = \left\{\frac{A+B}{Ax}\right\} \frac{\lambda}{2} dp .$$

Since for optimum visibility there should not be an inherent change of order greater than one fourth[35], the change in θ due to the mirrors not being optically flat must not be greater than,

$$\left\{\frac{A+B}{Ax}\right\} \frac{\lambda}{8} .$$

If a>>b

$$d\theta \ngtr \frac{\lambda}{8x}$$

That is, the optical tolerance is inversely proportional to the fringe width. The broader they are the more optically flat the mirrors must be.

If a=b $d\theta \ngtr \frac{\lambda}{4x}$

While the inverse proportionality still holds the tolerance on broad fringes is doubled.

If a<<b

$$d\theta \ngtr \frac{\lambda B}{8Ax}$$

Which means that for a given fringe width the tolerance is dirctly proportional to the distance of the eyepiede from the mirror M_2.

Therefore the best experimental conditions for viewing the fringes are

(a) Mirrors flat to one tenth of a fringe

(b) The primary slit at avery small distance from the fully silvered mirror. This can be effected by focussing a real image of the slit at some position close to the surface of the fully silvered mirror.

(c) The eyepiece at a large distance from the mirror system.

G. The Counting of Interference Fringes

At the time of writing the optical flats for the mirrors have not been completed. However, test runs using the original mirrors have shown that the counting of fringes can be successfully performed.

The output of the photomultiplier was, after amplification, fed into the trigger circuit of figure 23 which in turn was coupled to a scaler. Since the counting rate would not be much more than 20 fringes per second under normal conditions a high speed mechanical counter or a scale of two would be quite sufficient.

H. The Interferometer as a Refractometer

The most popular forms of Refractometer appear to be the Rayleigh and the Jamin.[36] Two others, namely the Mach-Zehnder[37] and the Michelson have been used but rarely.

The Rayleigh , Jamin , and Mach-Zehnder are similar in that they make use of Fresnel-like fringes. The Michelson , however, employs circular fringes at infinity. In any method the accuracy of a determination is dependent on the error associated with the estimation of the centre of a fringe.

The peculiar disadvantage of the Rayleigh arises from the use of two slits as the coherent sources. If these are separated by any great distance the fringes become extremely narrow . To some extent this is overcome by the use of a cylindrical eyepiece, which, since it magnifies only in one plane effects a great saving in light but even so, the slit separation limits the size of the gas holders.

Nevertheless, the great advantage of the Rayleigh lies in the use of a fiducial set of fringes. When any displacement in the working fringes has taken place, an angular displacement of a compensating plate returns them to coincidence with the fiduciary set. When monochromatic light is used the zero order fringe is identified with the aid of white light fringes. Moreover, this technique has the further advantage that it is independent of any change in the system as a whole. It is claimed that with practice a setting to one fortieth of a wavelength can be achieved. Again since the Rayleigh employs slits it can be easily used for extended measurements with a rich source, which is impossible with the other types where more or less broad sources are required.

The Jamin interferometer in which the coherent beams arise by refraction and reflexion also limits the separation of the gas holders. The chief difficulty is the one of making the plane parallel slabs of glass which must be uniform and of exactly equal thickness. Although the latter disadvantage, it is claimed,[38] has been overcome, the use of a cross wire setting limits the accuracy of the instrument not only through personal error but also through the fact that changes may have occurred in the system as a whole relative to the cross-wire.

The Mach-Zehnder interferometer which is designed about four plane parallel slabs of glass placed at the corners of a rectangle does not restrict the separation of the gas holders. However, like the Jamin, it requires that the glass slabs be accurately plane and of equal thickness. Although, there is no obvious reason why a fiduciary set of fringes could not be employed the method used is that of cross-hair settings.

Like the Mach-Zehnder the Michelson places no restriction on the separation of the gas holders but possesses the additional advantage that since the light passes twice through the holders it effectively doubles them. However, the use of circular fringes causes the determination of the fringe shift to be difficult since cross- wires or fiduciary fringes would not be practical.

It may be safely claimed that the Guest interferometer possesses the overall advantages of these refractometers without any additional complications. Since the Michelson mirror arrangement is employed, the fringe shift will be related to the the refractive index by

$$2(\mu-I)L = p\lambda$$

where, μ = refractive index

L = length of the gas holder

λ = the wavelength.

A fiduciary fringe system may be easily arranged and since a slit is used sources rich in lines can be accommodated. The fringe separation can be varied at will by a slight turn of one or both of the fully silvered mirrors.

Moreover since the light path is doubled the inherent accuracy is twice that of the Rayleigh. In addition since it is possible to count the fringe shift electronically and at the same time to record the distribution it may be possible by the use of very broad fringes to set on the centre of a fringe with a greater accuracy than one fortieth of a wavelength.

J. Conclusion

It may be possible, using techniques similar to those developed in the course of this work, to make a close study of two phases of Physics which are of both theoretical and experimental importance, namely,

(a) A redetermination of the Refractive Index of gases.

(b) Michelson Visibility Curves with regard to line broadening and fine structure

(a) In the first case, an accurate knowledgeof the refractive index of air has Spectroscopic applications. Again, there is still doubt as to the correct relation between the refractive index of a gas and its density especially when there is a temperature change. Moreover, there appears to be some connection between the refractive index of an element and its position in the periodic table.

A Refractometer using Fresnel fringes as in the Guest interferometer could be easily designed. The best arrangement would be that of Vautier, where the various components are mounted on separate stands. The stands carrying the fully silvered mirrors would need

(i) An arrangement for rotating the mirrors about a vertical axis.

(ii) Rightangled levels and level adjustments.

(iii) Screw travels which moved one mirror along a line perpendicular to the plane of its face and the other along a line parallel to the plane of its face. The length of travel need not be more than 2cms. The stands could then be set at any distance determined by the size of the gas holders.

(b) The Michelson Interferometer used as an instrument for studying the homogeneity of spectral lines has been considered obsolete for fifty years. However, if resolving power is considered to be the ability to interpret the form or distribution of the source and not the ability to distinguish completely the components of a source then, the Michelson theoretically possesses unlimited resolving power.

In essence, Michelson's method[39] consisted in making visual estimates of the clearness or visibility of the fringes at various path differences. The visibility was defined by,[40]

$$V = \frac{I_{max} - I_{min}}{I_{max} + I_{min}}$$

Where

I_{max} = intensity of light at the centre of a bright fringe

I_{min} = Intensity of the light at the centre of an adjacent dark fringe.

so that the fringes had the greatest clarity when V = I and the least when V = 0.

If the source were perfectly monochromaticthat is, the line was mathematically sharp, a plot of the visibility for various path differences would feveal a straight line. Since it is physically impossible to obtain a perfectly sharp line the visibilit curve observed is the resultant of those arising from a number of homogeneous sources of different intensities and frequencies. Hence, practical procedure requires the analysis of the observed curve into its Fourier components. Provided the original line or group of lines is symmetrical this will give a unique correct result.[4I] This analysis Michelson performed by means of his 'Harmonic Analyser'[42] and with it was able to infer the character of prominent spectral lines with an accuracy that has not been exceeded.

Shortly after 1900, the method lost face for reasons which are summarised best by Michelson himself.[43]

(a) '' It requires a very long time to make a set of observations and we can examine only one spectral line at a time.

(b) The method of observation requires us to stop at each turn of the screw and note the visibility of the fringes at each stopping place.

(c) During the comparatively long time it takes to do this the character of the radiations may themselves change.

(d) There is trouble translating the visibility curves into distribution curves . Hence it is easy for errors to creep in.

Apart from these objections the high resolution instruments that were developed about this time by Fabry-Perot and Lummer-Gehrcke led to its being discarded. Another difficulty with the method is that the circular fringes at infinity become very small when the path difference is large causing the visibility estimations to be even harder.

A method of surmounting this difficulty however, has been suggested by Williams[44]. He proposes the use of Twyman and Green fringes.[45] These fringes can be arranged to any convenient size and provided the ways on which the mirror moves are sufficiently true keep the same separation independent of the path difference, this is equally true of Fresnel fringes obtained by the method of section E.

Consequently, the photomultiplier tube lends itself to attempting a direct record of the visibility curve with simultaneous counting of fringes. Adapted to studying the complexity of spectral lines it would most probably be only of historical interest but may possess possibilities in the study of line broadening and the fine structure of Raman satellites.

CHAPTER IV

The Photoelectric Recording of Stellar Transits.

(A) Present Methods of Recording a Transit

(i) Introduction

When a star crosses the meridian the apparent sidereal time at that instant is equal to the stars Right Ascension (RA). Consequently, the determination of time is limited by the accuracy with which the RA of the star is known. Conversely, the accuracy with which the RA of a celestial body can be calculated is fixed inter alia by the accuracy with which the sidereal time is known.

The transit instrument is especially designed for such work. It is a refracting telescope which has in the focal plane of its eyepiece an odd number of vertical wires. Its mounting is such that it is free to move only in the plane of the meridian and ideally, the central wire always lies in this plane. In practice, the observer watches the passage of a star across the field and defines the instants that the star is bisected by a cross hair by transmitting pulses to a chronograph which simultaneously, is receiving signals from the clock.

These observations are usually made on the brighter stars, called the clock stars, whose transits have been recorded over many years. The accuracy of their positions has been repeatedly improved by successive approximation so that by using them to determine the transit instant, the error of the clock can be inferred. Consequently, if the rate of the clock be calculated by observations of the same star on consecutive nights the differences of RA between pairs of stars can be obtained. Thus, a series of differences of RA can be obtained. In this manner , with any given instrument, a series of star places can be observed and by comparing observations at different epochs the proper motions of the stars can be deduced.

The advance in the means of keeping time has been such as to outstrip the means by which it is determined. The pendulum and crystal clocks now in use are such that intervals of time can be measured to within a few parts of a millionth of a second. On the other hand, the internal probable error of a transit observation is at least ten milliseconds.

Although these clocks have extremely high precision they are not freefrom sudden changes of rate and small irregular fluctuations in rate. These irregularities which may be of the order of I0 to 20 milliseconds cannot be determined accurately by observations which may be in error by as much as 50 milliseconds and which are spaced irregularly with sometimes gaps of days. It follows that any marked improvement in the accuracy with which stellar transits are recorded would lead to a better control of these irregular fluctuations.

(ii) The Sources of Error

The principal sources of innacuracy associated with time determinations are due to

(a) Instrumental Errors

(b) The Observer

While instrumental errors in most cases are the chief source of error attempts are being made to design instruments which reduce them to the second order.[46] Indeed, the Zenith tube[47] in which the instrumental errors are reduced to a minimum has been in use for a number of years.

Nevertheless, the inaccuracies associated with the observer may vary from night to night or even during the course of a series of observations. They can be ascribed to two causes.

(i) The Personal Equation

(ii) The Magnitude effect.

(i) The Personal Equation

The most popular transit instrument[48] makes use of an ''impersonal '' micrometer eyepiece. As the star moves into the aperture the observer bisects it with a guide wire and follows it across the field. The guiding can be either manually controlled or motor driven with the observer manipulating a fine control. At intervals defined by the revolution of the drive , electrical contact is made and the pulses fed to the chronograph.

The personal error has been ascribed to[49]

(a) Bisection Error

(b) Following Error

The former arises when the wire is set to the right or left of the centre of the image, irrespective of the direction of motion of the star in the field. Provided the angular error of bisection is independent of the speed of the star , this error is proportional to sec δ , where δ is the declination The latter occurs if in the observation of the moving image the wire is systematically set either in front or behind the centre of the image. It also varies as sec δ .

For the majority of observers the bisection error is larger than the following error . Where the greatest accuracy is desired , it is necessary to determine the absolute personal equation of the observer. This may be done by a personal equation machine which makes use of an artificial star.[50]

(ii) The Magnitude Effect

This effect is systematic and depends on the brightness of the star observed, faint stars being judged correspondingly late compared to bright ones. It is peculiar to the tap method of observing and is of very little importance if an impersonal micrometer is used. The equation is also a function of sec δ.

In order to overcome these sources of inaccuracy there have been many attempts to design entirely impersonal instruments. While many possess distinct advantages they themselves tend to introduce new errors and are in general complicated and expensive arrangements. As has been mentioned, the photographic zenith tube has proved the most successful of these attempts. Its disappointing feature however, is that it requires the observation of stars much fainter than the standard clock stars which means that their positions are not so accurately known.

It would be a distinct advance if some means of impersonally recording a stellar transit could be developed. The Photomultiplier offers a solution which if successful could be easily and economically adapted for use with existing instruments.

(B) Stellar Magnitudes VIsible to a Photomultiplier tube attached to a 5½'' Refractor.

If it is to be possible to follow up the ideas of Chapter I the Photomultiplier tube must be capable of giving easily detectable currents from the clock stars, which arbitrarily will be assumed to be not less than the 6th magnitude. The tubes used in this work were found to possess a dark current of the order of 10^{-13} ampere so that in the following discussion this value will be assumed. It is also inherent in the discussion that the multiplier is being operated with sufficient overall voltage to make the noise level a function only of the cathode current and the seeing conditions. Consequently using the results of Chapter II the signal to noise ratio is given by

$$\left(\frac{S}{N}\right)^2 = \frac{I_{s'}^2}{\left\{\frac{m}{m-1}\pi e\left(I_t+I_s\right)+A I_s^2 \sec \zeta\right\} f_0} \quad \text{---- (i)}$$

Consideration of the dimensions of equation (i) shows that A must have the dimensions of Time. One figure given for A at Mt Hamilton U.S.A. is 2 x 10^{-3} seconds.[51] This from the point of view of order corresponds to values of 10^{-2} seconds at Utrecht.[52] From personal observations on a Cathode Ray Oscillograph at Sydney the scintillation frequency appears to be of the order of hundredths of a second. Consequently, a value of 10^{-2} seconds for A will be assumed.

Now there will be some value I_ℓ of I_s for which

$$\frac{m}{m-1}\pi e\left(I_t+I_s\right) f_0 = A \sec\zeta\, I_\ell^2 f_0$$

That is,

$$I_\ell = \frac{2.13\times10^{-19}}{2A\sec\zeta}\left\{1+\left(1+\frac{4I_t A\sec\zeta}{2.13\times10^{-19}}\right)^{\frac{1}{2}}\right\} \text{ ampere} \quad \text{-- (ii)}$$

Since the sensitivity of the Sb-Cs surface of the 931-A is about 10 μampere per lumen equation (ii) may be written in terms of luminous flux as

$$Q_\ell = \frac{2.13\times10^{-14}}{2A\sec\zeta}\left\{1+\left(1+\frac{4I_t A\sec\zeta}{2.13\times10^{-19}}\right)^{\frac{1}{2}}\right\} \text{ lumen} \quad \text{-- (iii)}$$

If 'm' be the magnitude of a star and 'D' the aperture in inches of the telescope then, the light flux in lumens is given by[53]

$$2.5\log_{10} Q = 5\log_{10} D - m - 22.43 \quad \text{-----(iv)}$$

Therefore,

$$m_\ell = 5\log_{10} D - 22.43 - 2.5\log_{10}\left[\frac{2.13\times10^{-14}}{2A\sec\zeta}\left\{1+\left(1+\frac{4I_t A\sec\zeta}{2.13\times10^{-19}}\right)^{\frac{1}{2}}\right\}\right] \quad \text{(v)}$$

Specifically, this means that for stars smaller in magnitude than 'm_l' the tube noise limits the accuracy of measurement. On the other hand when magnitude of the star is greater than 'm_l' the precision is determined by the degree of seeing. This limit may be reduced by

(a) Increasing the aperture of the telescope

(b) Decreasing the thermionic dark current

(c) Confining observations to stars of fairly high altitude.

When D = $5\frac{1}{2}$'' and $I_t = 10^{-13}$ ampere the seeing noise of a 5.8 magnitude star will be equal to the phototube noise while reducing the dark current to 10^{-15} ampere requires an 8.1 magnitude star to set the same condition.

It follows therefore, that for stars of magnitude much greater than 'm_l' equation (I) becomes

$$\frac{S}{N} = \frac{1}{\sqrt{A f_0 \sec \zeta}} \qquad \text{(i.a)}$$

Also since the reciprocal of the relative root mean square error of measurement is equal to the signal to noise ratio the probable error of a measurement is given by,

$$\epsilon = 0.6745 \sqrt{A f_0 \sec \zeta} \qquad \text{(i.b)}$$

This means that on a particular night, for a given declination the probable error is independent of the magnitude of the star but directly proportional to the band width of the measuring equipment.

On the other hand for stars less than 'm_l'

$$\frac{S}{N} = \frac{I_s}{\left\{2.13 \times 10^{-19} (I_t + I_s) f_0\right\}^{\frac{1}{2}}}.$$

so that, for a given band width the probable error of a single observation increases with zenith distance in case A but with increasing magnitude in case B.

Since the minimum stellar magnitude visible with a telescope of aperture D is given approximately by ,

$$m \doteq 9 + 5 \log_{10} D$$

the minimum magnitude visible with a 5½'' refractor is I2.7. Consequently, the calculated value of m_l is well within the visible limits of the telescope, and although the efficiency of the multiplier is only half that of the telescope it will give recognisable outputs from stars of the sixth magnitude or greater.

Since the efficiency of the Multiplier is a function of the bandwidth of the following amplifier and the dark current of the tube it can be considerably increased by reduction of one of both of these factors.

In photometers where use is made of light chopping methods or the incident beam is from an AC source the band width is determined by that of the AC amplifier. The noise equations differ only by the introduction of a modulation factor. It is possible to design such an amplifier with a bandwidth of I cps [54] and with special regard to stability even as low as 0.I cps[55], but this appears to be the ultimate limit.

With a direct current method the band width is equal to one quarter the reciprocal of the delay constant of the galvanometer, while in an integrating method where condensers are charged it is equal to the reciprocal of the time of charging. If long time constants are satisfactory then the band width can be made very small. Again , if electron counting is employed the band width can be made as small as one pleases since it is inversely proportional to the time of a count.

Each and every one of these methods can be used for work with low levels of light.

By its very nature , however, the transit problem precludes the use of an integrating method. Since it is concerned with instants a direct coupling method must be used. This necessity was the cause of the principal difficulty.

(C) The Telescope and its alignement

The telescope on which all this work was performed was a $5\frac{1}{2}$'' refracting equatorial. It was erected on the Western tower of the Physics building where, except for a few dgrees of arc to the south, the night sky could be covered from horizon to zenith.

The equatorial mounting has two degrees of freedom. One describes the declination circle; the other traces the hour circle. When aligned correctly the setting of the two circles at values derived from star charts of tables places the celestial object in the centre of the field of view.

Briefly, the aligning involved

(a) Rough setting of the polar axis in the plane of the meridian and levelling of the pillar.

(b) Fine adjustments on recognisable stellar objects lying in the meridian and equatorial planes.[56]

For our work an accuracy of some thirty seconds of arc in declination and some thirty seconds of time in hour angle were deemed satisfactory. With these, reliable settings could be made.

(D) Photomultiplier Tube Housing and Accessories.

To deliver the high tension a conventional voltage doubler was built. It was capable of delivering II00 volts minus. The output of the doubler was fed to a stabiliser and as finally operated the voltage per stage could be varied between 60 and I00 volts. These circuits are considered in more detail in Appendix I.

The tube housing is based on the

designs of Strong, Kron and Bowe. Figure 24 is a drawing of the housing while figures 25 and 26 show it attached to the telescope. The steel Bowden-like cable held the supply leads to each dynode and plugged into the stabiliser. The anode lead was a separate shielded wire.

(E) Astronomical Observations

(i) Preliminary

The initial observations were by means of a moving mirror galvanometer. The method followed in most of this work was to set the telescope a little off the star in H.A. with the driving clock going. The tube housing was swung into line with the eyepiece, clamped, and the light tight cover slipped into place. When the instrument had been adjusted the clock was stopped and the passage of the star watched by its record on the galvanometer. The nett result of the preliminary observations indicated that some amplification of the current was necessary if the transit of faint stars was to be attempted.

The amplifier chosen was in basic a Bridge type direct-coupled circuit which allowed the balancing out of both the dark current and the night-sky background.

More transits were now recorded. The recording instrument in this case was a microammeter. The responses were encouraging but were found to contain two complications,

(i) As the star moved lengthwise along the cathode pulses of current were exhibited.

(ii) As the star moved widthwise across the cathode the number of pulses was reduced but the tube was effective for only part of the field of view.

It was obvious that the pulses were due to the disappearnce of the image behind the wire grid-like shield placed by design, in front of the cathode. This shield is made up of a number of wires zigzagging along the length of the cathode which explained the greater number of pulses coming from a lengthwise stellar movement. As can be seen from figure 27 , the ideal position of the cathode is at the plane of the exit pupil, for in this position the minimum movement of the image during a transit occurs.

This could be arranged by projecting the exit plane of the eyepiece onto the plane of the cathode. The simplest way of doing this was found to be the setting of a two lens cell in the tube between the eyepiece and the cathode. The focal length of the lens was designed to be a quarter of the distance between the cathode and the exit pupil. It was placed so that, as closely as possible the centre of its principal planes was half way beteen them. In suah a position the exit pupil of the telescope was imaged on the cathode at unit magnification. This meant that the angle subtended by the cathode width at the centre of the exit pupil was now much greater than the apparent field of view of any of the available eyepieces.

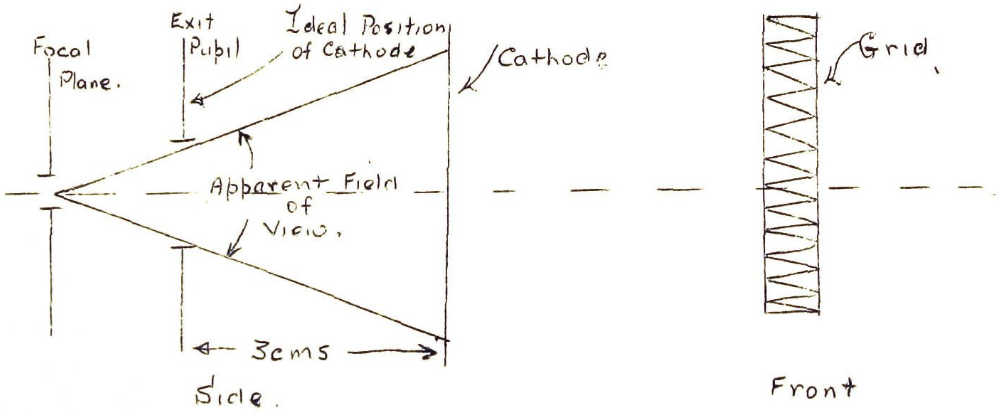

fig 27

Consequently, by setting the tube housing so as to give a widthwise movement of the stellar image across the cathode not only was the tube effedtive over the whole of the field but also the pulses were eliminated.

To test the effect without recourse to night observations an artificial transiting apparatus was devised. An artificial star, consisting of a pinhole in front of the slit of a spectrometer served the purpose. The tube housing was mounted on a lathe travel and the light-tight cover slipped over the eyepiese of the spectrometers telescope. The table of the spectrometer was covered with a dark cloth making the pinhole the only source of light. With this arrangement, screwing of the lathe travel took the telescope with it and the resultant effect was similar to stellar motion across the field. No pulsesfrom the shield were seen and since the field of view of this eyepiece was much greater than those of the telescope the optical system was considered to be satisfactory.

(ii) Cross Hairs.

In order to observe the effect of a star passing behind a cross hair, several of them were placed in the focal planes of the eyepieses of the spectrometer and the telescope. The output of the amplifier was taken to the Y plates of a Cathode Ray Oscillograph.

Since quite definite kicks were obtained with the artificial transits night observations were recommenced. The procedure was essentialy the same as before the only change was to balance out the night sky before the clock was stopped.

The nocturnal observations revealed that the laboratory transits had been performed at much too great a rate. In practice,a complicated noise pattern appeared on the screen as the star entered the field of view while the passage of a star behind a cross hair resulted in a slow return to the condition giving a quiescent trace. As the star re-appeared so did the noise without any sign of a kick.

The amplitude of these fluctuations was up to 75% of the mean intensity. Although, the time occupied by a single fluctuation was quite random it was of the order of a few hundredths of a second. They were similar for stars of different magnitudes and occurred even when the image as seen through the telescope seemed steady to the eye.

Up to now the aim had been to obtain pulses the rise and fall of which would be fast enough to enable the instant of bisection by a cross hair to be determined from them. It had become obvious that if the method was to succeed the pulses would have to be sharpened and the efeet of stellar scintillation reduced. In an attempt to do this the three stage direct coupled amplifier of fig 28 was built. It was so designed that when the star was in the field the amplifier was biassed beyond cut-off. It was hoped that as the star went behind a cross hair the time of switch to the'no signal condition would be small compared to the scintillation frequency. In actual practice the intensity distribution appeared somewhat like figure 29

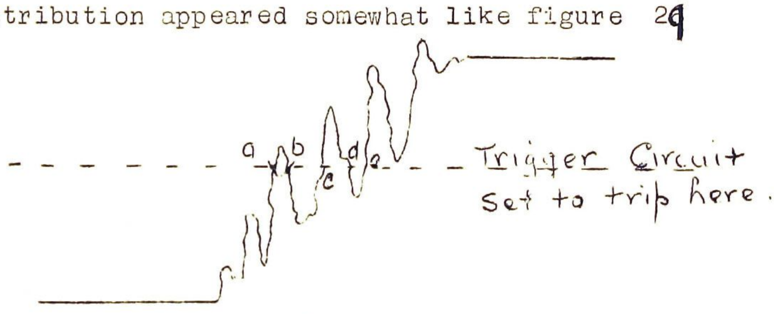

fig 29

If the rise time of the pulse could be made small in comparison with the intensity fluctuations due to twinkling then it would be possible to trip a trigger circuit at some point in the rise and fall of the pulse as outlined in chapter I. It was obvious that any such attempt with the distribution of the above figure would result in spurious pulses from the trigger circuit at such points as 'a', 'b', 'c' etc.

With the classical method of recording a transit, direct coupling gives a negative output pulse which for the majority of the time is complicated by noise. On the other hand the use of a biassed amplifier gives positive pulses the rise and fall of which are slow when compared to the scintillation frequency. It was felt that if positive intensity pulses were used some hope of success might be entertained. As a consequence, it was decided to replace the ' cross hair - biassed amplifier' arrangement with an opaque graticule on which fine lines had been ruled. Since the width of these lines would be small the cathode would be energised only so long as some part of the stellar image were on the slit. When the star was behind the opaque portions of the graticule the output of the Photomultiplier would be zero.

(iii) The Use of a Slit Graticule

The graticules were designed as in figure 30 In the first place a chemical silvering method was tried to give the required opacity. Although smooth edged slits could be ruled with this coating trouble from pin holes led to it being discarded in favour of a black lacquer. The lines were ruled on this while it was wet. On some of them side windows were left to facilitate the sighting and the

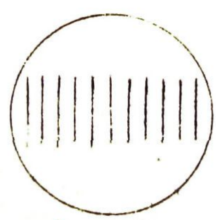

fig 30.

focussing of the star. They were placed in the focal plane of the Huygenian eyepieces.

Observations were recommenced using these graticules and in addition the highly stable direct coupled amplifier of figure 9, which our previous work had revealed as a necessity. The output of this amplifier was placed on the 'Y' plates of the Cathode Ray Oscillograph. Althoughthe pulses appeared a lot sharper they were still complicated by noise and since it was difficult to decide the true nature of the pulse it was decided to record them on a Chronograph.

The cathode ray spot was focussed by means of a photographic objective onto sensitised paper fixed to a drum which revolved with a peripherial speed of the order of a centimetre per second. Figure 31 is a typical trace recorded by ϵ Pegasi (m = 2.54). In the bottom trace the gain of the amplifier was set to overload and give a flat top. In the other trace, which is of the same star, the gain was reduced below the overload value. Fortunately, the particular night chosen happened to be one of extremely poor seeing conditions and figure 32, which is the trace of α Aquilae clearly reveals the effect of scintillation. Figure 33 is another trace of ϵ Pegasi obtained by revolving the drum by hand at a speed sufficient to resolve the twinkling. Its random nature is evident. These traces clearly show that any attempt to trigger a pulse would be unsuccessful.

However the records, even as they stand represent a good statistical average. For example if the four points 'A' 'B' 'C' and 'D' on each pulse are considered a probable error of $0.I \times (4n)^{-\frac{1}{2}}$ seconds where 'n' is the number of pulses would result, since these points may be quite easily read to 0.I seconds. In fact for this particular trace the probable error is about 22 milliseconds. In order to facilitate the readings time markers, consisting of 0.2 second pulses were fed onto the same plates as the signal. In addition graticules possessing more lines were prepared.

Renewed observations gave tracks such as figure 34. There are nine traces in track I and

and I9 in track 8. The separation in the latter case is really too small and begins to approach the crosshair method where the star is energising the cathode for longer than it does not.

Besides the twinkling difficulty another factor, which hitherto had not been considered was shown to be important if not the most important effect. It was the size of the stellar image. The ideal case of Chapter I is based on the movement of a source of uniform brightness. While, the image by its very nature could never satisfy this condition a good objective would produce an image consisting of a bright central maximum surrounded by several weaker maxima. The image produced by the $5\frac{1}{2}$" refractor was poor with chromatic and comatic aberration predominating. The objective was checked and found to be improperly centred. After alignment it was put back into position. Although, there appeared to be a slight improvement the image was still poor and to effect further improvement the objective was stopped down to approximately 2". While this was rewarded with further success the image was still far from ideal.

The type of trace resulting is shown in figure 35. Unfortunately, it was a very windy night and since the telescope was unprotected the dancing of the image from vibration sometimes occurred in the direction of motion of the star producing a sharp pulse as at 'B'.

However, seeing conditions aside these traces revealed that any attempt to fulfill the aim of Chapter I would be unsuccessful. Nevertheless the traces even as they stand can be read to a probable error of IO to 30 milliseconds which is of the same order as the visual methods and only a little greater than the photographic zenith tube.

Conclusion

Although it cannot be claimed that the method is entirely successful there are several features which make it not wholly unsatisfactory. While the scintillation effect appears to be the predominating difficulty the real 'bête noir' is the size of the stellar image, due to the poor optics possessed by the telescope. Even traces such a sfigure 3b present a very good average from which a transit estimation with a probable error of 30 milliseconds may be quite readily obtained. Since the image is so poor the rise time of the pulse is slow because the cathode begins to be energised long before the central maximum of the image is reached. It follows that with a well defined image this rise time would be reduced. With proper bias the secondary maxima would not be recorded. This increase in the slope of the pulse would most certainly lead to a reduction in the noise. Consequently, a transit instrument possessing good optics should under good seeing conditions produce pulses on which particular points could be read to less than 0.1 seconds. Even for this estimate an eyepiece which could accomodate 16 slits and a record on which six readings per pulse were made would infer an errorof 10 milliseconds. If internally consistent this would represent a distinct advance. It might even be possible to determine the exact form of the intensity distribution which in comparison with the observed distribution over a series of observations might lead to a recognition of internal consistencies, and a further increase in the accuracy.

Besides considerations of accuracy the impersonality of such a method has desirable features. Errors arising from observational fatigue and physiological and methodical differences between observers would disappear.

Since it is well within the capability of a Photomultiplier tube to produce working currents from those stars the positions of which are accurately known the disadvantage of the Photographic Zenith tube would be overcome. Moreover its ability to detect such stars without refrigeration means that its mounting on any telescope would be relativelly simple and light.

While this attempt, as it stands cannot be said to be completely successful, it is felt that even with its inherent difficulties the photoelectric recording of stellar transits is feasible. Further work under better optical and positional conditions might prove it to be quite practicable.

Appendix

The Electronic Circuits

The various chapters

indicate that the accent in this work has been stability at low frequencies. The logical approach to low fbequencies is by means of direct coupled circuits. Unfortunately, direct coupling from its very nature introduces instability. Moreover, besides wishing to count at low frequencies, the desire to record the instant of transit withheld the normal procedure of current integration. Consequently, regulation and stabilization had to be introduced to a high degree.

(A) The Power Supply

The Photomultiplier requires some I000-I200 overall volts. To supply this the conventional voltage doubler circuit of figure 37 was built. The voltage delivered was negative with respect to ground. The rectifying tubes were Mercury filled of Japanese design and to guard against accidental contact in the dark the whole supply was completely enclosed in a sheet metal cover.

Besides inherent noise , fluctuations in gain due to variations in the supply can become troublesome. To reduce this effect two stabilization devices are employed. The first is an instantaneous mains stabilizer known as the 'Stabilac S I000 B/2 @. This ensures an input supply to the doubler which is independent of variations in the main.

The circuit of Figure 38 stabilizes the output of the doubler. It is essentially that of Dieke, and works on the regenerative amplifier principle. A Potentiometric control allows a dynode voltage variation of about I0 volts per stage. The voltage per stage can be varied between 60 and I00 volts per stage by shorting the required number of VR I50 'tubes.

@ Manufactured by Stabilac Propriety Ltd. 49 York St. Sydney

The stabilisation was of the order of I% for a 20% input variation which although not as good as expected was sufficient for the developemental work.

The feed to the phototube was by separate lead to each dynode. The IO leads were enclosed in a steel Bowden-like cable some 20ft long and directly attached to the tube housing. The photographs of the housing in position on the telescope show part of it. A separate shielded anode lead was used to cut down as much as possible on the leakage paths.

It is now felt that a series of dropping resistors about the pins of the socket is a better way of supplying the tube. It has proved quite satisfactory in another application in the department. It was found that by removing the anode lug from the socket and attaching the lead directly to the anode pin a reduction of the order of IO in the dark current occured. Removal of the anode pin altogether has been advised but this was never tried.

(B) Amplifiers.

During the developemental work three different approaches were made to the problem of subsidiary amplification. In order the circuits were

(a) Bridge Type

(b) Biassed Type

(c) Negative Feed Back Type

(a) The Bridge Type Fig.37

It is highly desirable when using the Photomultiplier with direct coupled circuits to have some means of balancing out the direct component of the dark current. In this type zero balance was effected by the use of matched 6J7G tubes arranged in a bridge circuit. The gain proving insufficient an A,C stage was later added through long time constants. Although it proved useful in the early work its stability as can be seen from figure 6 was very poor.

(b) Biassed Amplifier Figure 28

The difficulty arisng out of twinkling led to the design of this amplifier. By means of the I megohm input potentiometer the bias could be adjusted to compensate for the different stellar magnitudes. When compensation had been effected the voltage of the cathode of the 6B6 was adjusted by means of the 10K potentiometer until the tube cut-off. This gave a quiescent trace on the Cathode Ray Oscillograph while the star was in the field. As the output of the Photomultiplier dropped due to the eclipsing effect of the cross hair the 6B6 tube began to draw current. The exact position where this occured depended of course on the bias setting. Its stability however was questionable and as has been explained the method was unsuccessful.

With fringe counting in mind the extra EL3NG power stage was added. It was intended to use it to make and break a mechanical counter.

(c) Negative Feed Back - Push Pull Type Fig 9

This circuit is based on one used by Kron[58] for stellar photometry. It possesses its own regulated power supply which delivers the necessary +240, +108 and -100 volts. Regulation is achieved by a regenerative amplifier arrangement which causes any change in the 240 volts output to be reflected as a change of potential of opposite sign at the plate of the 6J7G which applied to the grid of the 6V6 leads to compensation for the initial change.

The amplifier itself is a three stage direct coupled circuit with each component in the primary side matched by a component in the secondary side.

Originally, there was only one double triode of the 6SN7 type. It was found however, that if the meter resistence fell below IOK ohms the amplifier became unstable. This instability was reduced by putting another 6SN7 in parallel, and the meter acrossit. This in effect separates the output stage from the feedback and balance stage.

The amount of negative feedback can be controled by the series of resistors arranged about the feedback switch. The minimum gain and maximum feedback occurs when there is a high resistence across the switch which means that the amplifier is most stable when the gain is least. The dark current is balanced out by means of the potentiometer P_1 while slight mis-matches in the components are balanced out by means of P_2. The input components are well shielded to reduce instability due to pickup.

Owing to the high dark current of the Photomultipliers used a complete balance could not be achieved in the high gain positions.when the IO megohm input resistor was employed. It was found necessary to include a subsidiary battery potentiometer.

(c) The Trigger Circuit Fig 23

The trigger circuit is a direct copy of the one described by Yu[59]. It is a direct coupled regenerative amplifier possessing two stable states. Plate current flows in only one tube at a time and can be caused to transfer abruptly from one tube to the other. Its peculiar advantage is that it can be directly coupled to a leading circuit and the switching takes place as soon as a critical input voltage is reached. It triggers on when this voltage is reached and off at a value a little below it. The particular circuit shown gives a 50volts output pulse for a difference of input voltage of as little as ½ volts.

This is the circuit that was used in the trial runs of fringe counting, Its ability to deal with input frequencies of a few cycles per second makes it the most important tool of the fringe counting technique. A modification suggested by Yu which enables the circuit to be set to trigger on and off at the same point on the input pulse was being built at the time of writing. It will be used in the further developement of the fringe counting programme.

——————......——————

BIBLIOGRAPHY

(I) Dieke, Lohe & Crosswhite J.O.S.A. 36, 185, 1946

(2) Nahstoll & Bryan J.O.S.A. 35, 646, 1945

(3) J.O.S.A. 38, , 1948

(4) Rank, Phister & Coleman J.O.S.A. 32, 390, 1942

(5) Zworikin, Malter & Morton Proc. IRE 24, 351, 1936

(6) Janes & Glover RCA Rev. 6, , 1943

(7) Allen J.S. Proc. IRE 38, 346, 1950

(8) Sommer & Turk J.Sc.Inst. 27, 113, 1950

(9) Pearson G.L. Bell Syst. Tech. J. 13, 634, 1934

(10) Strong J. "Procedures in Experimental Physics" (Prentice Hall Inc. N.Y. 1944)

(11) Kron G.E. Pub. Astr. Soc. Pacific 52, 250, 1940

(12) Johnson H.L. Astrophysical J. 107, 34, 1948

(13) Danjon & couder " Lunettes & Telescopes" Paris 1935

(14) Wood R.W. " Physical Optics " MacMillan Co. N.Y. (3rd Ed.) 1934

(15) Wolson C.H. " Traite de Physique " Paris 1909

(16) Hartridge H. Nature 164, 999, 1949 & 165, 146, 1950

(17) Minnaert and others Nature 166, 151, 1950

(18) Hartridge H. Nature 166, 151, 1950

(19) Peterson & Holland J.O.S.A. 40, 253, 1950

(20) Saunderson Caldecourt & Peterson J.O.S.A. 35, 471, 1945

(21) Minnaert & Houtgast Zeits. fur Astrp. 10, 86, 1935

(22) Bowe P.A.E. Thesis Deg. M.Sc. Univ. Sydney 1949

(23) Shockley & Pierce Proc. I. R. E. 26, 321, 1938

(24) Engstrom R.W. J.O.S.A. 37, 420, 1947

(25) Sommer & Turk J.Sc. Inst. 27, 113, 1950

(26) Marshall Coltman & Bennet Rev. Sc. Inst. 19, , 1948

(27) Post & Shiren Phys. Rev. 78, 81, 1950

(28) Kallman & Accardo Rev. Sc. Inst. 21, 48, 1950

(29) Vautier Journ. de. Physique p888, 1903

(30) Handbuch der Experimentalphysik 18, Leipzig, 1928

(31) Jenkins & White " Fundamentals of Physical Optics" (McGraw Hill N.Y.) 1937

(32) Ignatowsky W. Annalen der Physik 23, 895, 1907

(33) Meyer C.F. "Diffraction of Light, X-Rays and Material Particles" Univ. Chicago Press 1934

(34) Michelson A.A. Am. J. Sc. p216 , 1890

(35)
(36) } Williams W.E. "Applications of Interferometry" Methuen Pub.

(37) Schardin H. Zeits. fur. Instrument. 52-53 , 424, 1932

(38) Kuln & Wheatley J. Sc. Inst. 22 , 130, 1945

(39) Michelson A.A. Phil. Mag. 34 , 280 , 1892

(40) Michelson A.A. Phil. Mag. 31 , 338 , 1891

(41) Rayleigh Phil. Mag. 34, 407, 1892

(42) Michelson A.A. " Light Waves and their Uses" 1903 (Univ. Chicago Press)

(43) Michelson A.A. "Studies in Optics" 1927 (Univ. Chicago Press)

(44) Williams W.E. Applications of Interferometry .

(45) Twyman F. Phil. Mag. 35 , 49 , 1918

(46) Spenser-Jones H. Proc. Roy. Soc. 198 , 141 , 1949

(47) Hellwig J.F. Pub. Ast. Soc. Pac. 52 , 17, 1940

(48) Struve. Astr. Nach. 155, 353 , 1901

(49) Spencer - Jones H. Reports on the Progress of Physics" 1v , 1 , 1937

(50) Spencer - Jones H. Reports on the progress of Physics" 1v , 7 , 1937

(51) Johnson H. L. Astrophys. Journ. 107 , 34 , 1948

(52) Minnaert & Houtgast Zeits fur Astrop. 10 , 86 , 1935

(53) Strong J. Procedures in Experimental Physics " (Prentice Hall Inc. N.Y.) 1944

(54) Terman F.E. Radio Engineers Handbook p943 (Mc Graw Hill Book Co. N.Y. 1943)

(55) Michels & Curtis Rev. Sci. Inst. 12 , 444 , 1941

(56) Challis H. " Lectures on Practical Astr." Cambridge 1879

(57) Kron G.E. Electronics 21 , 106 1948

(58) Yu Y.P. Proc. I.R.E. 37 , 1046 , 1949

Fig 6

Experimental Plot of Fresnel Biprism Pattern showing effect of zero drift of Amplifier

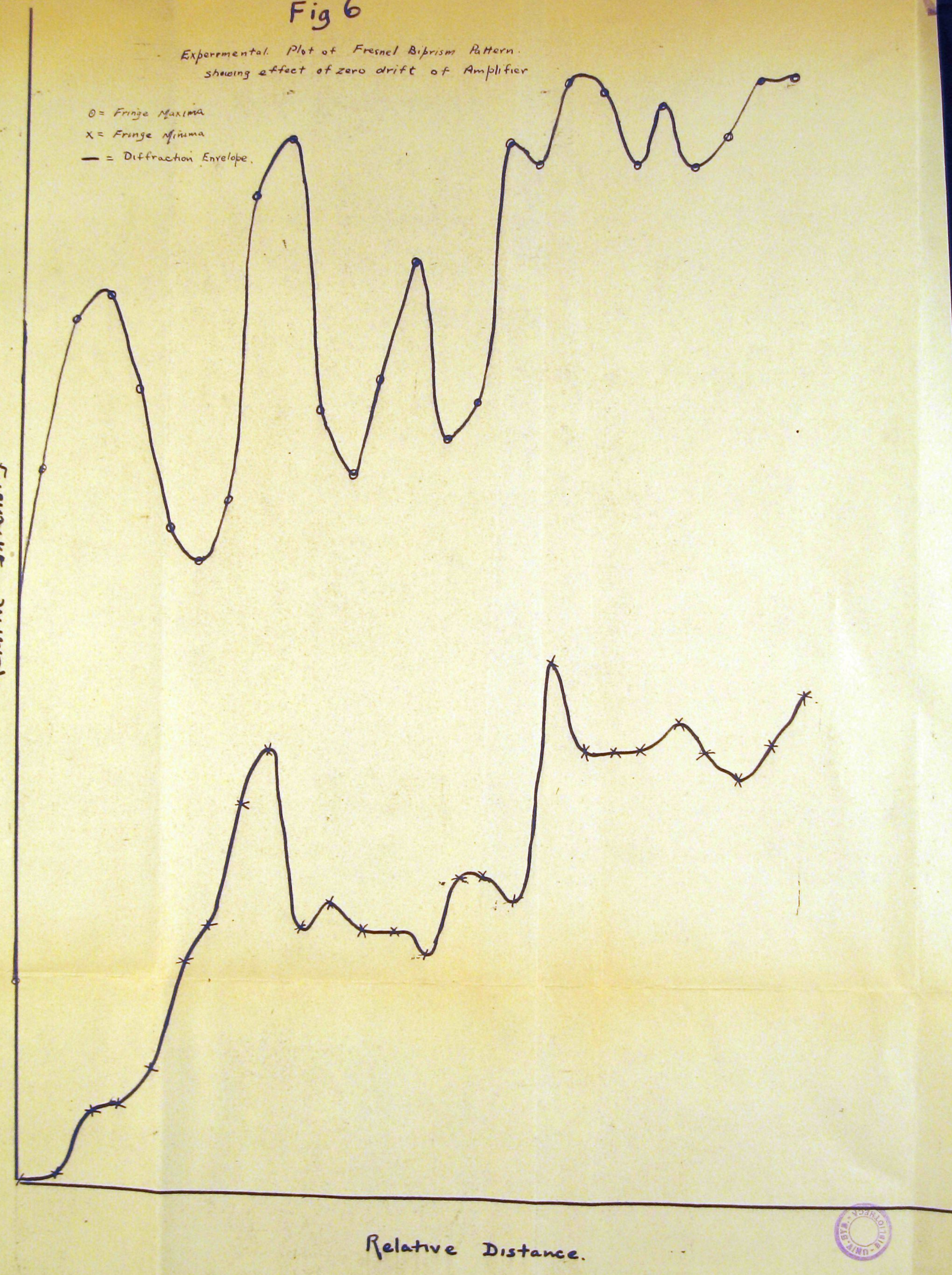

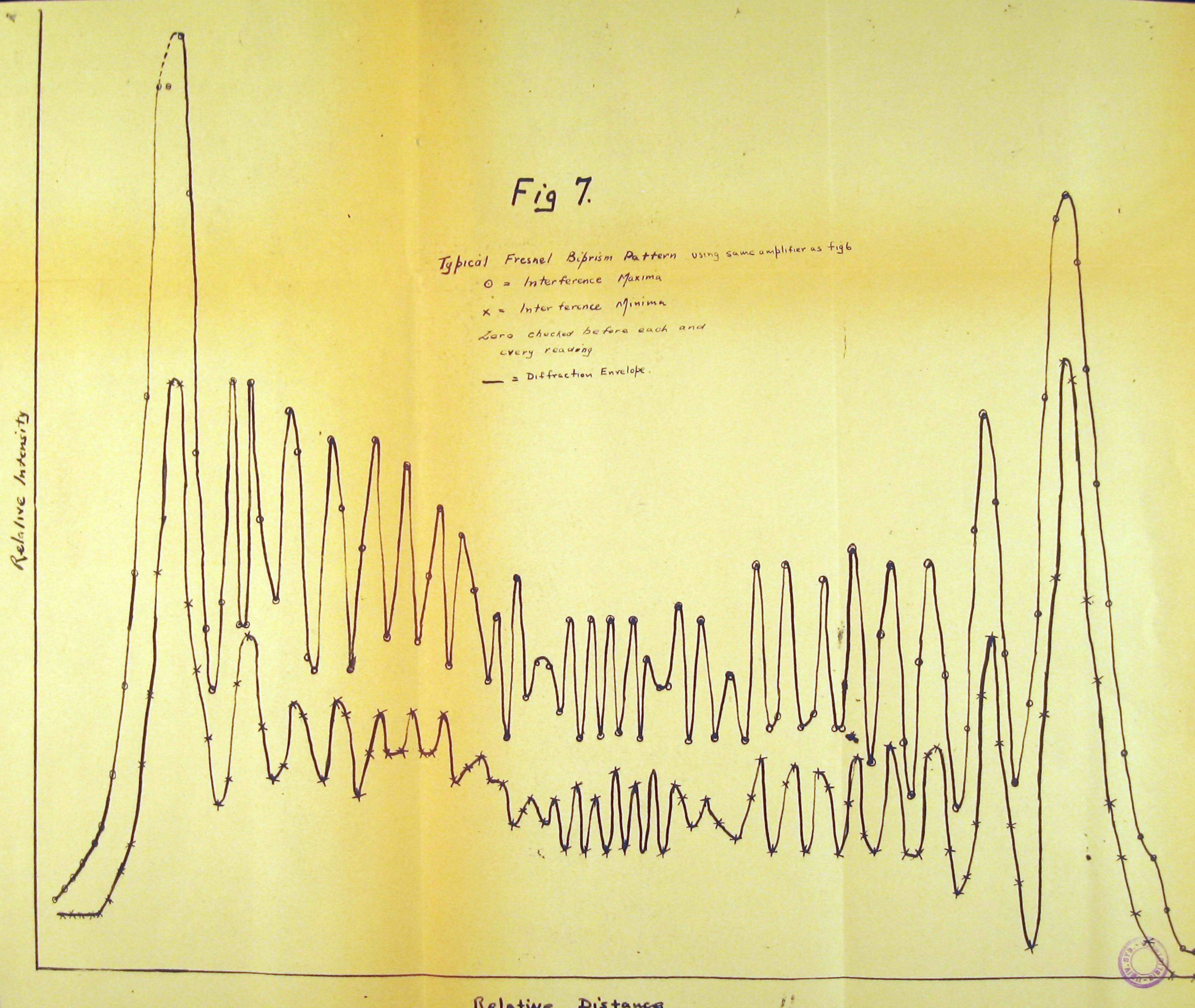
Typical Fresnel Biprism Pattern using same amplifier as fig 6
O = Interference Maxima
x = Interference Minima
Zero checked before each and every reading
— = Diffraction Envelope.
Relative Intensity
Relative Distance

Fig 7.

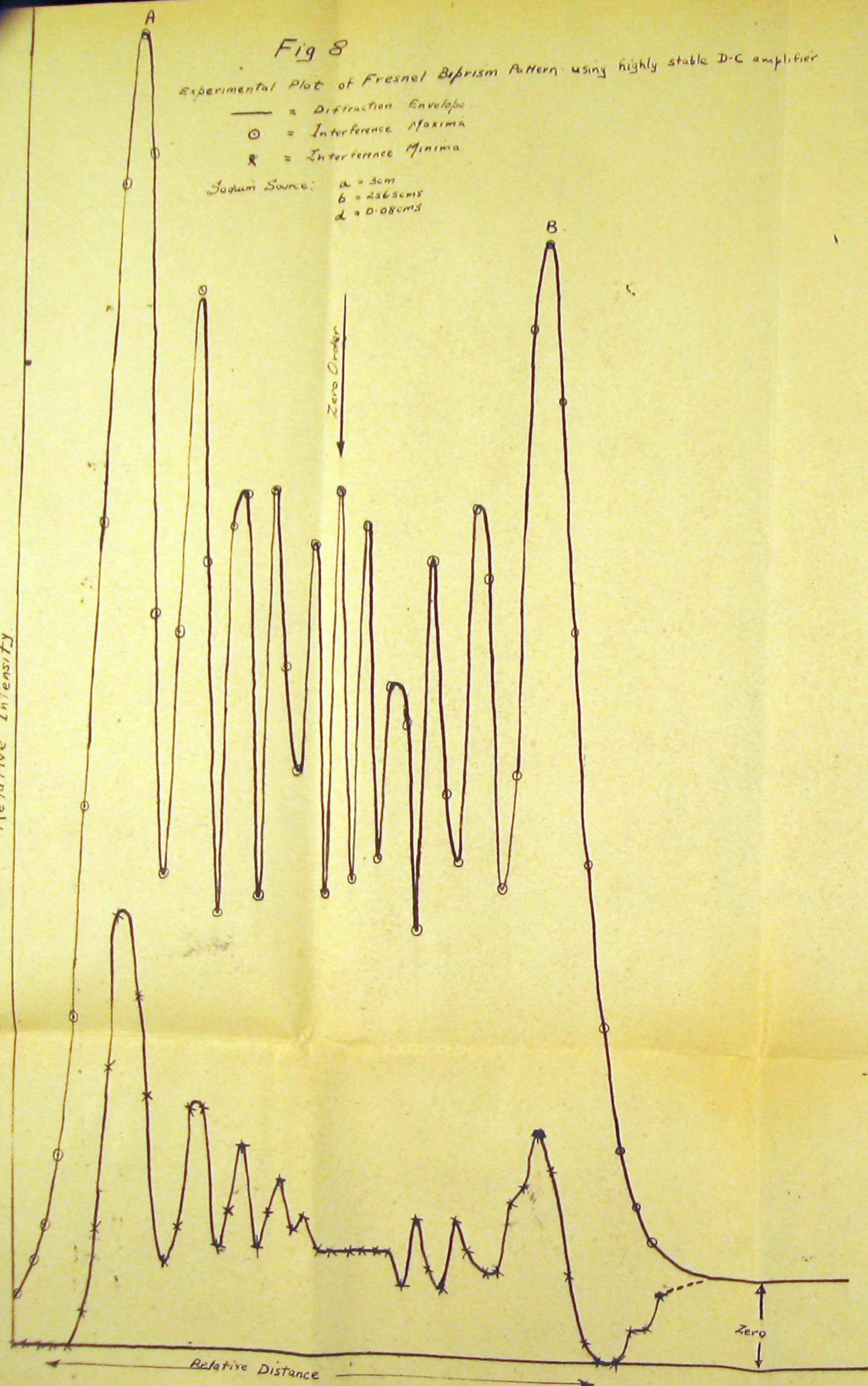
Fig 8
Experimental Plot of Fresnel Biprism Pattern using highly stable D-C amplifier
= Diffraction Envelope
⊙ = Interference Maxima
x = Interference Minima
Sodium Source: a = 3cm
b = 256.5cms
d = 0.08cms
A
B
Zero Order
Relative Intensity
Zero
Relative Distance

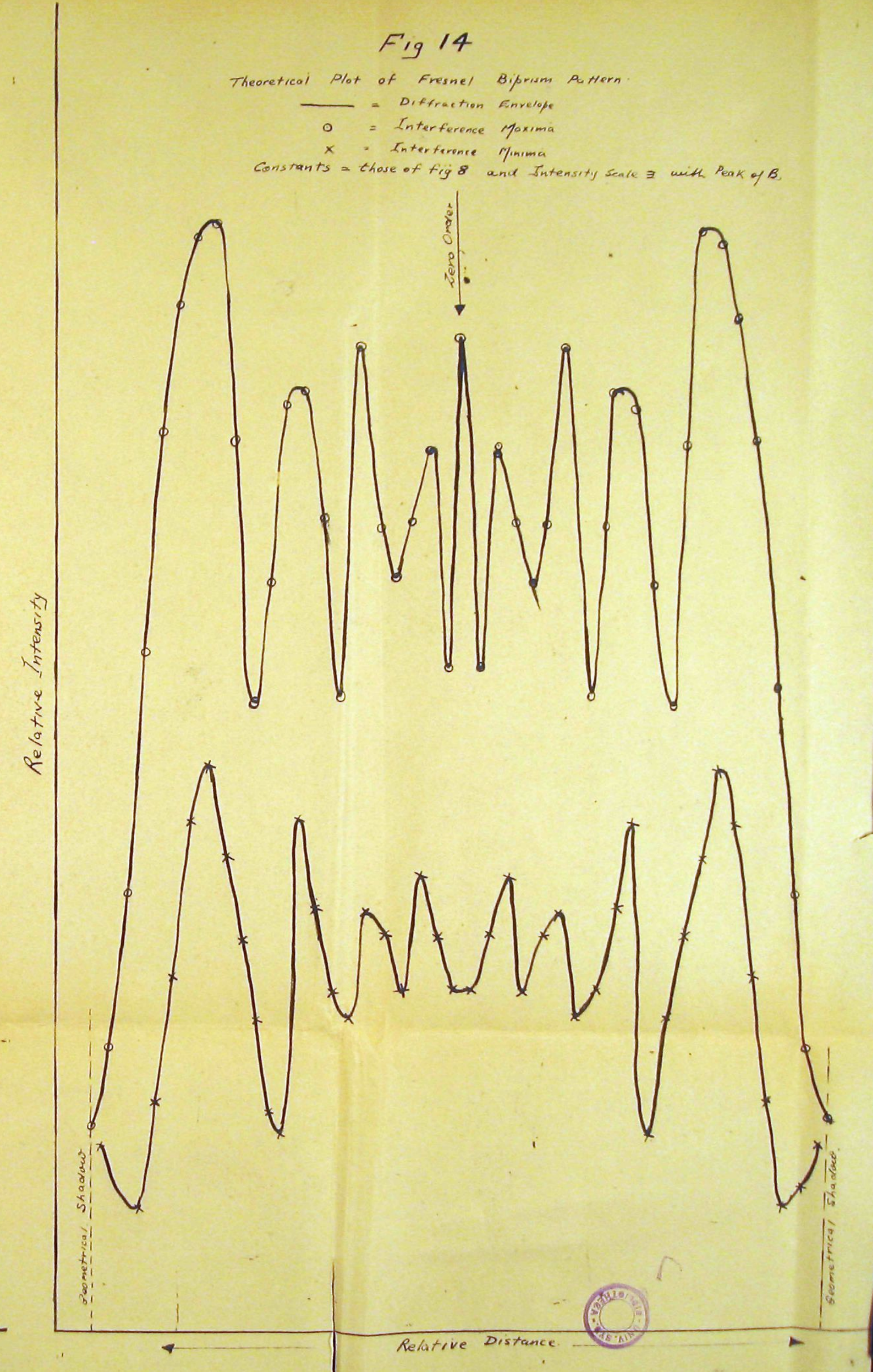
Fig 14
Theoretical Plot of Fresnel Biprism Pattern
= Diffraction Envelope
o = Interference Maxima
x = Interference Minima
Constants = those of fig 8 and Intensity Scale ∃ with Peak of B.
Zero Order
Relative Intensity
Geometrical Shadow
Geometrical Shadow
Relative Distance

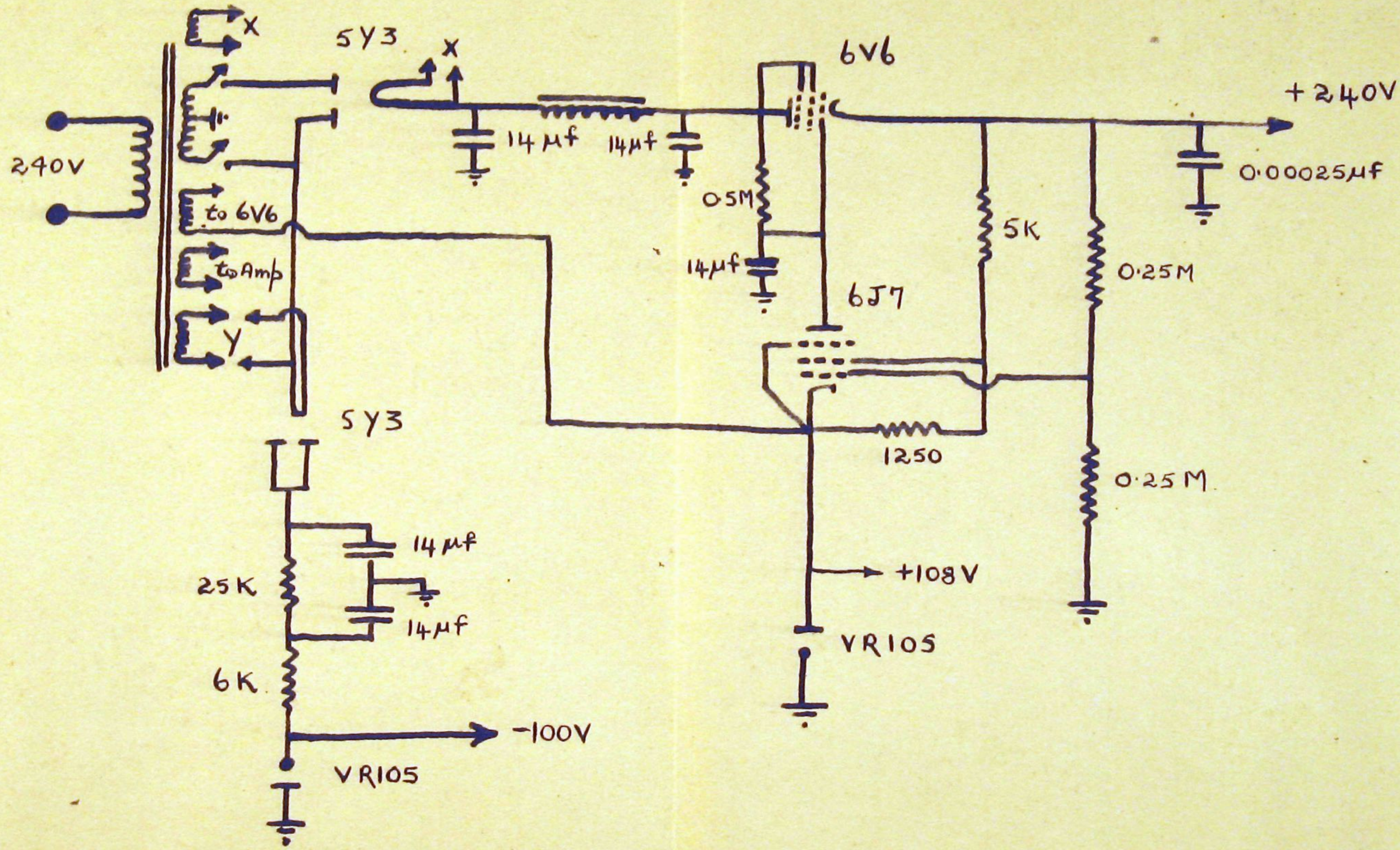
X
5Y3
X
6V6
+240V
240V
14μf
14μf
to 6V6
0.5M
0.00025μf
5K
to Amp
14μf
0.25M
6J7
Y
5Y3
1250
0.25M
14μf
25K
+108V
14μf
VR105
6K
-100V
VR105

Fig 9a

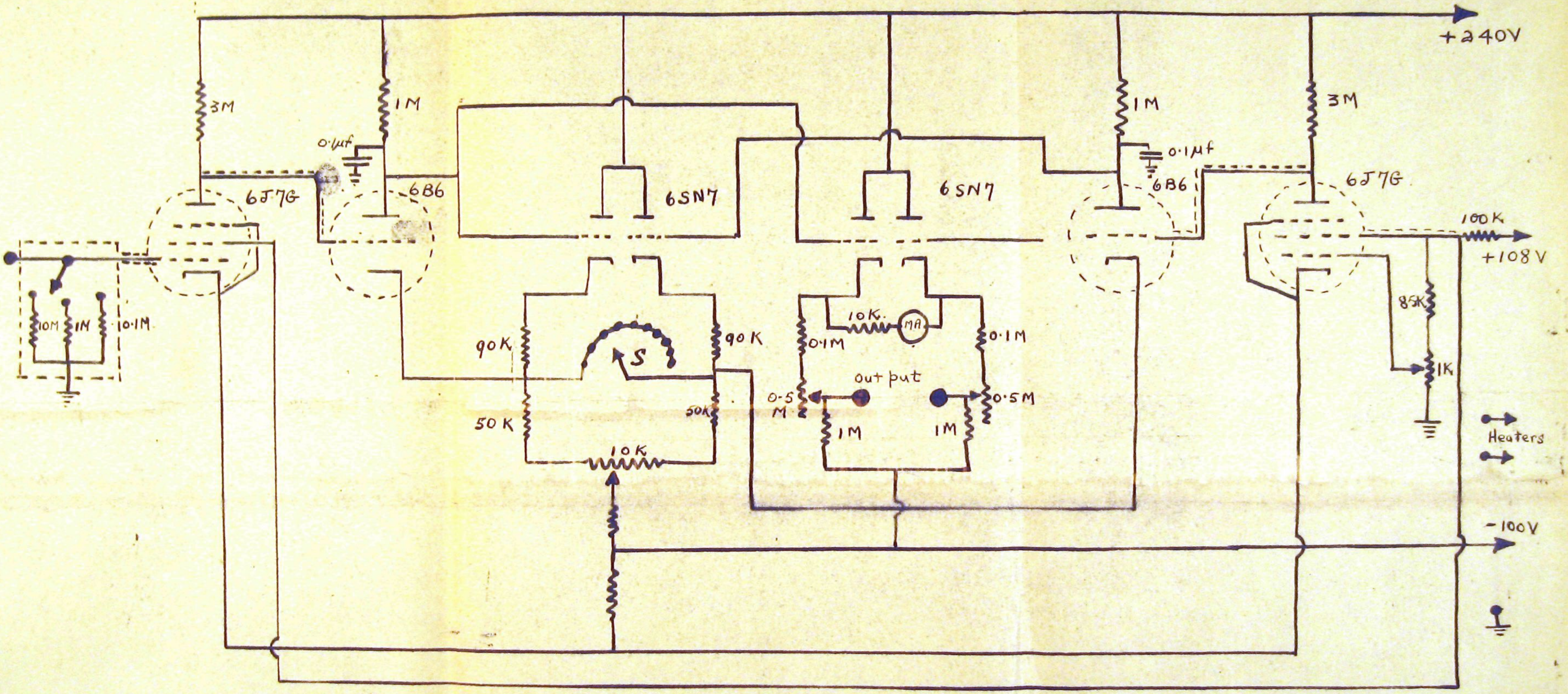
+240V
3M
1M
0·1μf
6J7G
6B6
6SN7
6SN7
1M
0·1μf
6B6
3M
6J7G
100K
+108V
10M
1M
0·1M
90K
S
90K
10K
MA
0·1M
0·1M
output
0·5 M
0·5M
50K
50K
1M
1M
85K
1K
Heaters
10K
-100V

Fig 9b

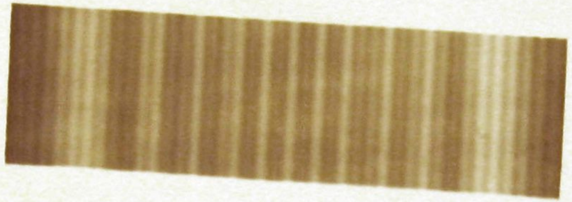

Fig 10

fig 11

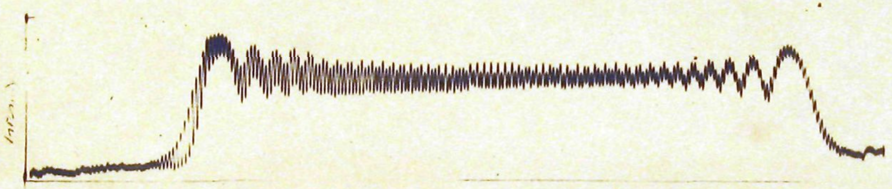

Fig. 3. Moll Microphotometer Trace
Fresnel Biprism Pattern.

Source light λ = 5893 Å.
Distance slit-plate 115 cm
Distance biprism-plate 45 cm.

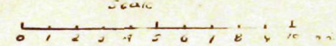

Fig 12

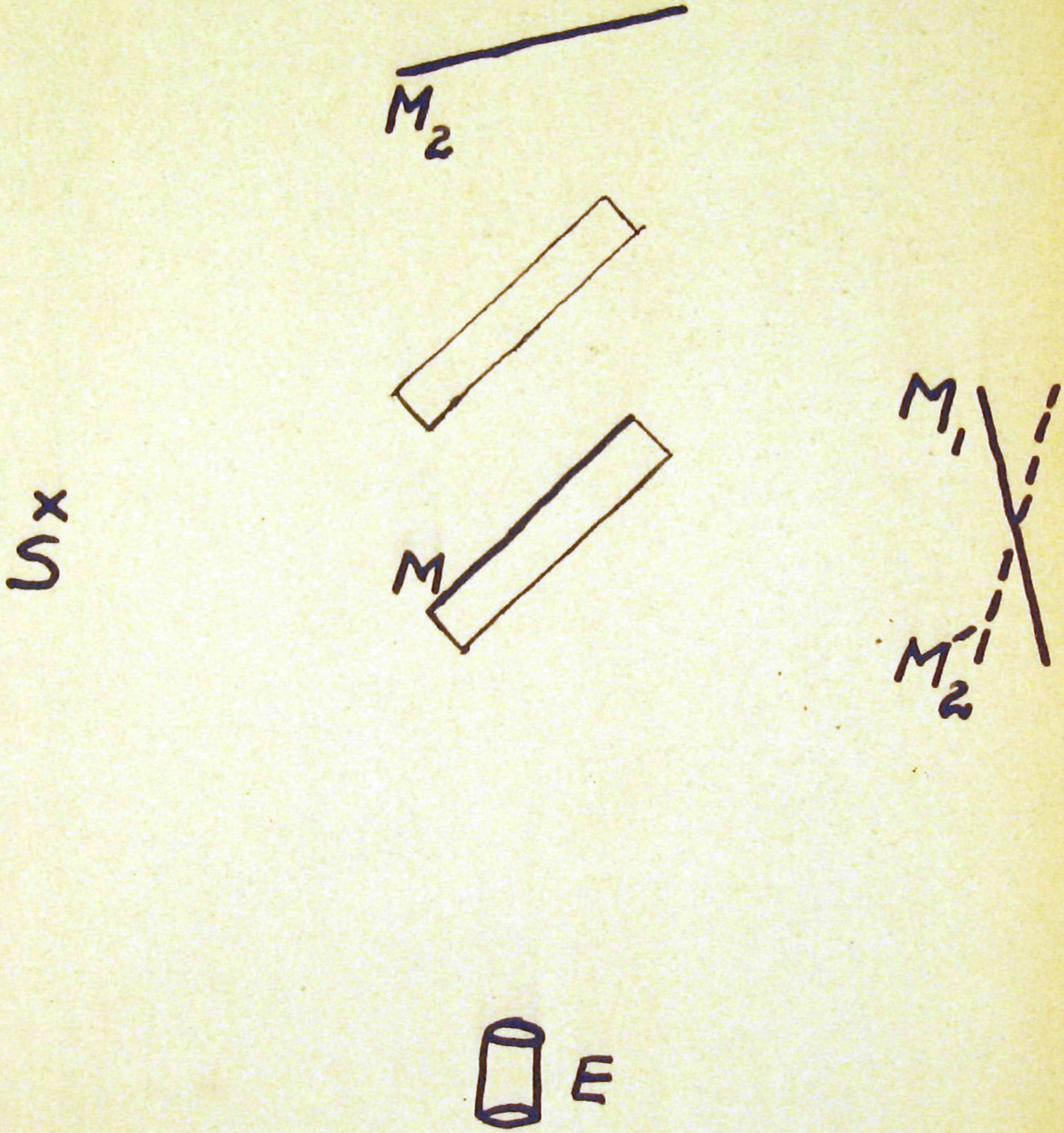

Fig. 15

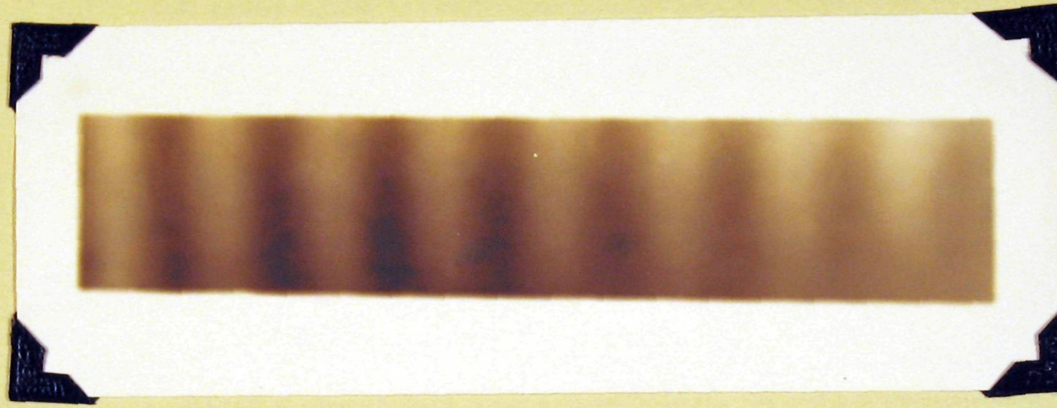

Fig 16

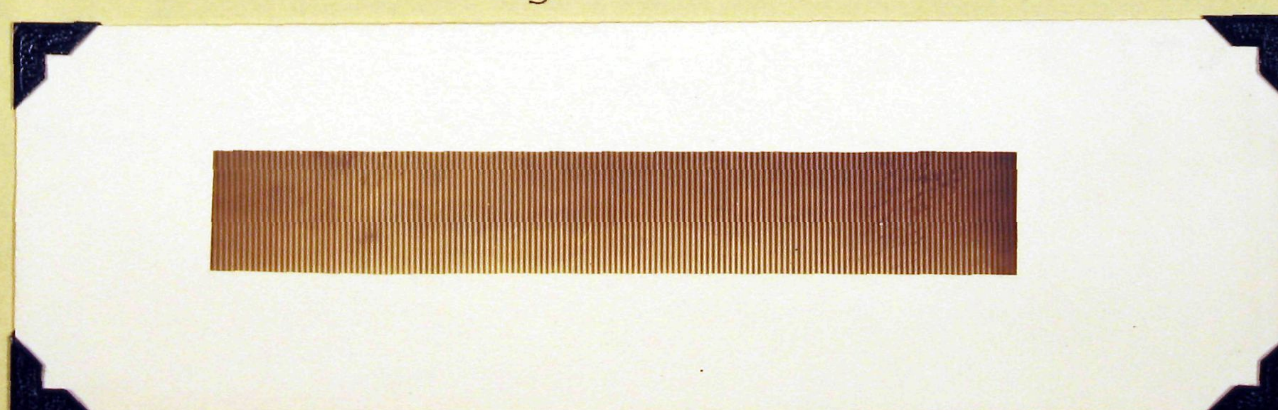

Fig 17

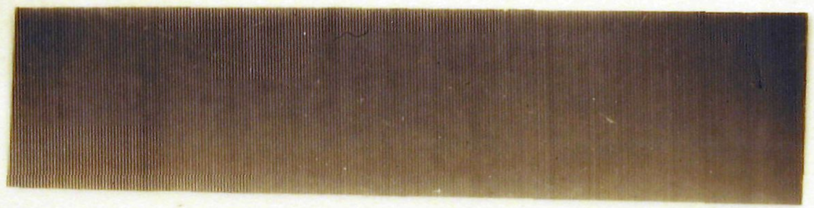

Fig 18

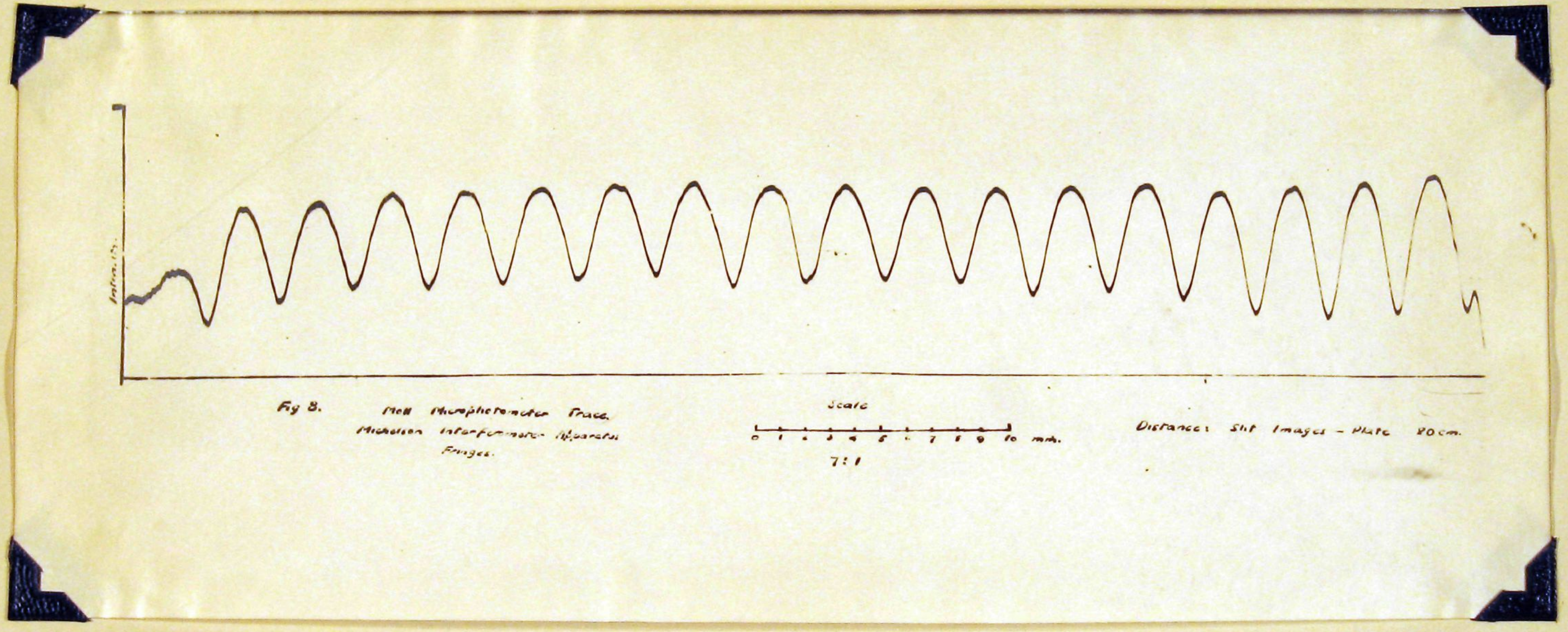
Intensity
Fig 8.
Moll Microphotometer Trace.
Michelson Interferometer Apparatus
Fringes.
Scale
0 1 2 3 4 5 6 7 8 9 10 mm.
7:1
Distance: Slit Images – Plate 80 cm.

Fig 19

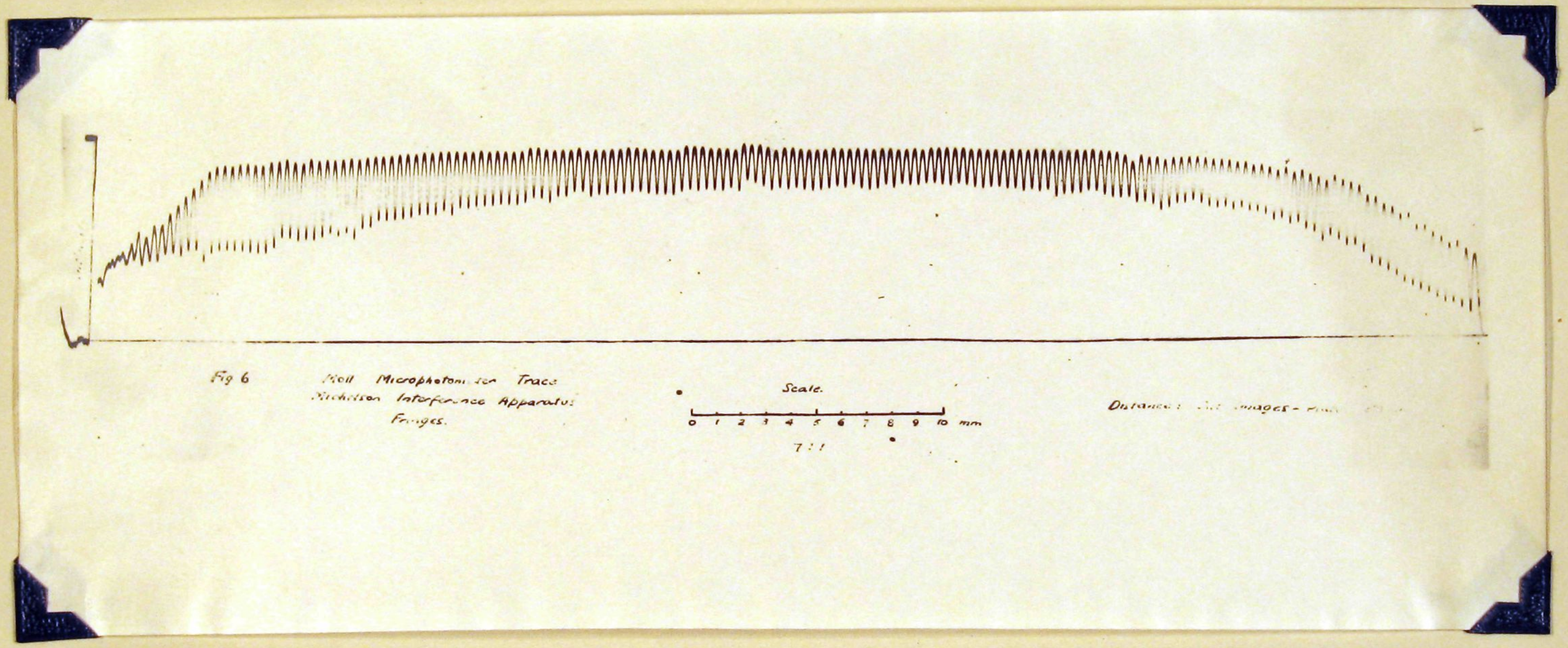
Fig 6
Moll Microphotometer Trace
Michelson Interference Apparatus
Fringes.
Scale.
0 1 2 3 4 5 6 7 8 9 10 mm
7:1
Distance : images -

Fig 20

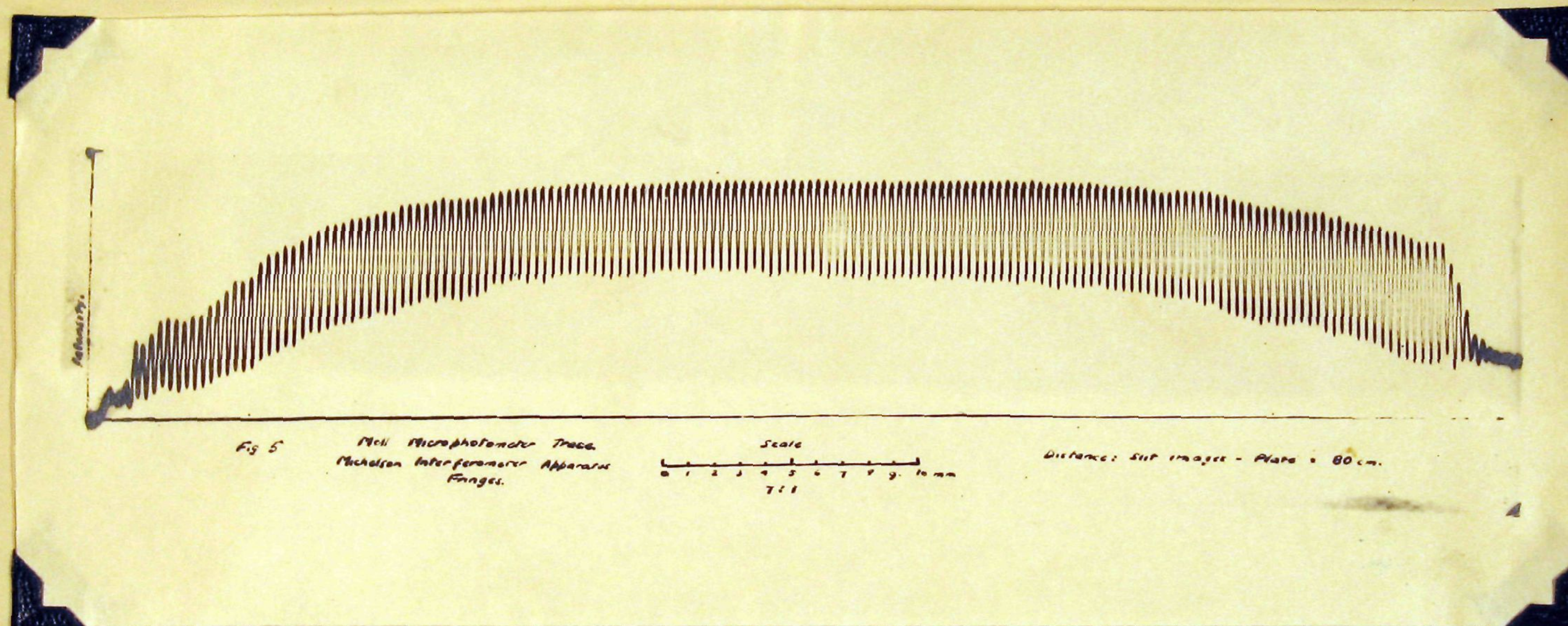
Intensity
Fig 5
Moll Microphotometer Trace.
Michelson Interferometer Apparatus
Fringes.
Scale
0 1 2 3 4 5 6 7 8 9 10 mm
7:1
Distance: Slit images - Plate = 80 cm.

Fig 21

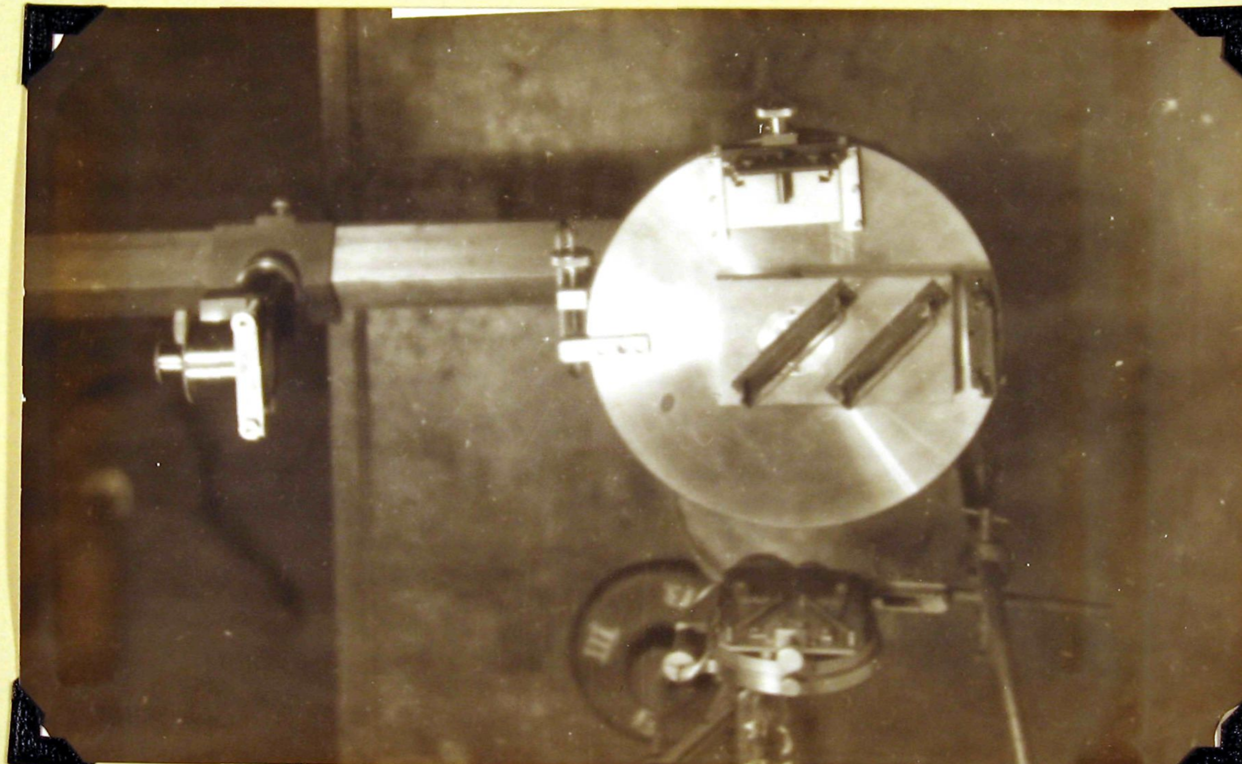

Fig 22a

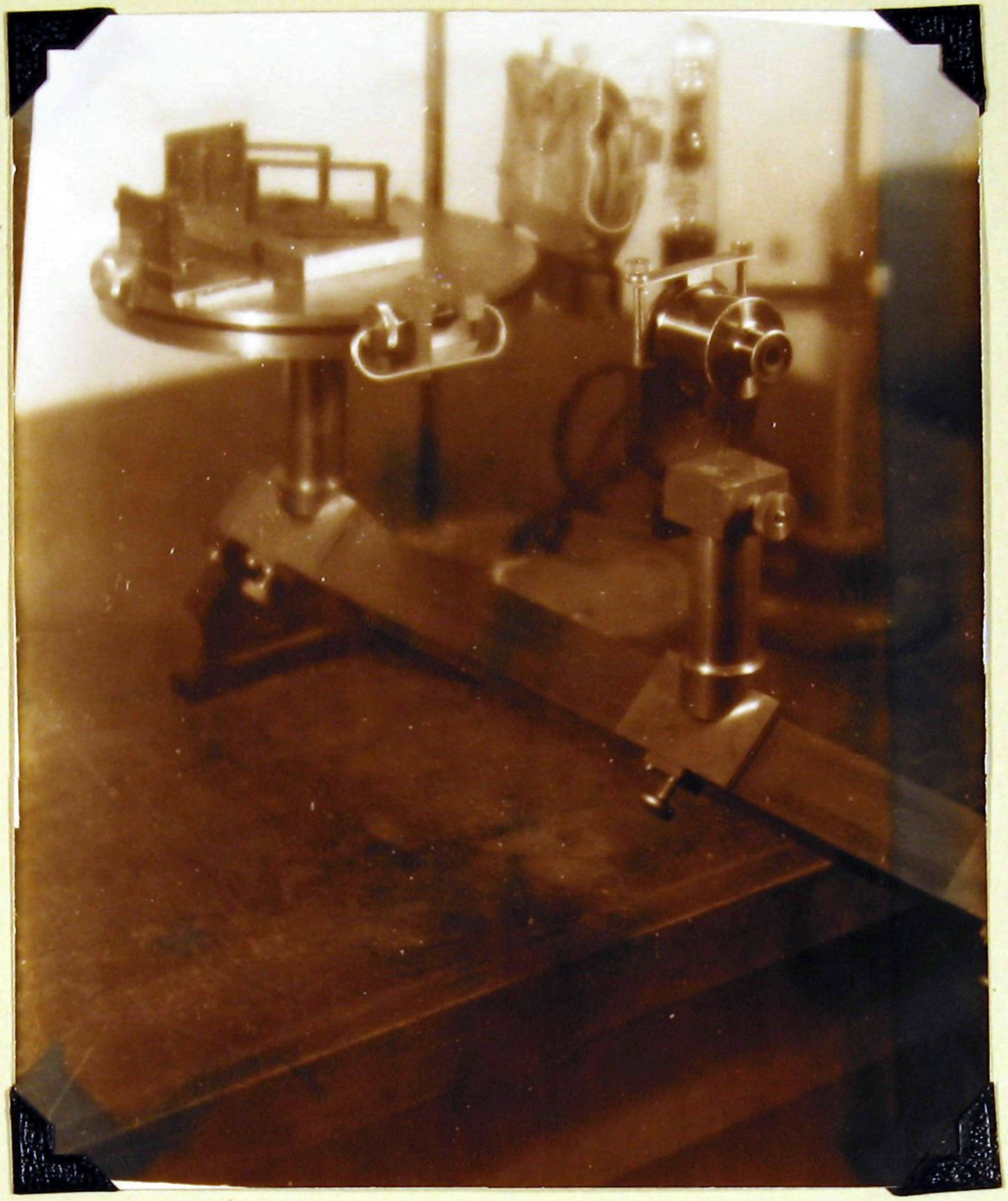

Fig 22b

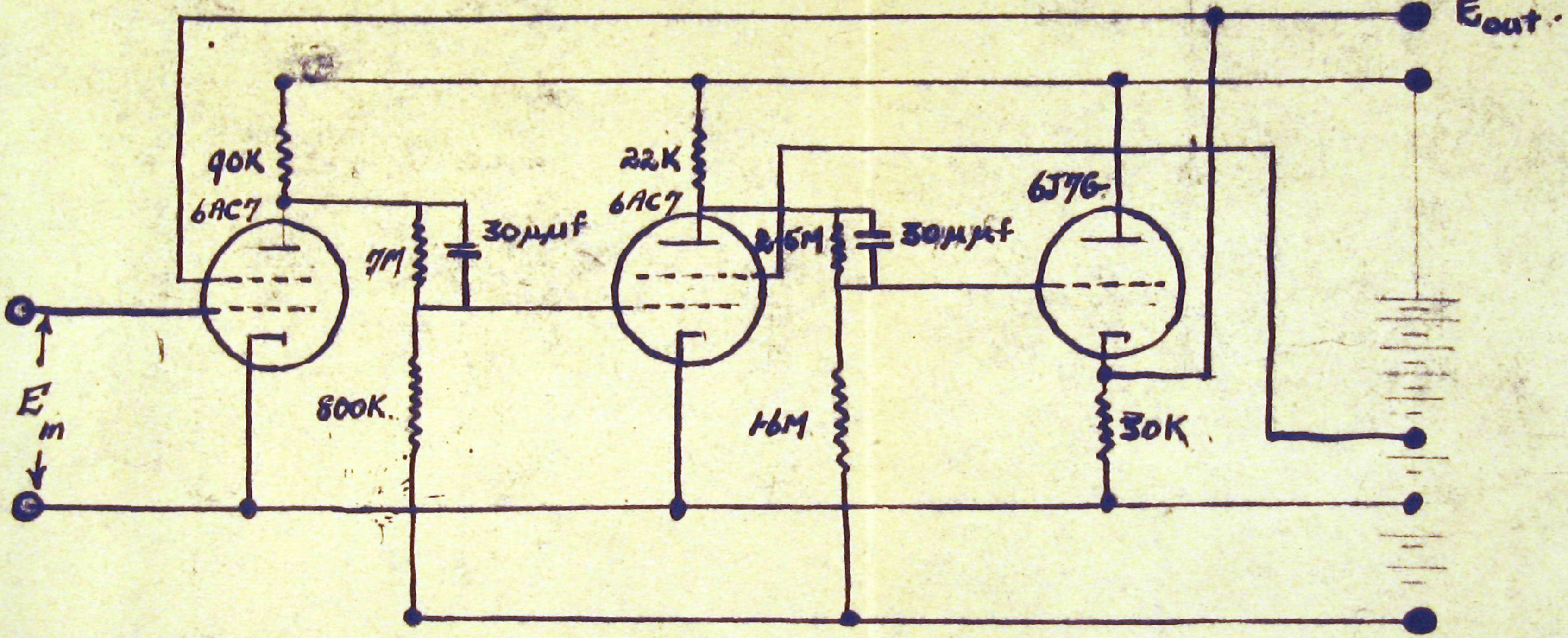
E out.
90K
6AC7
7M
30μμf
22K
6AC7
2.5M
30μμf
6J7G
800K
1.6M
30K
E in

Fig 23.

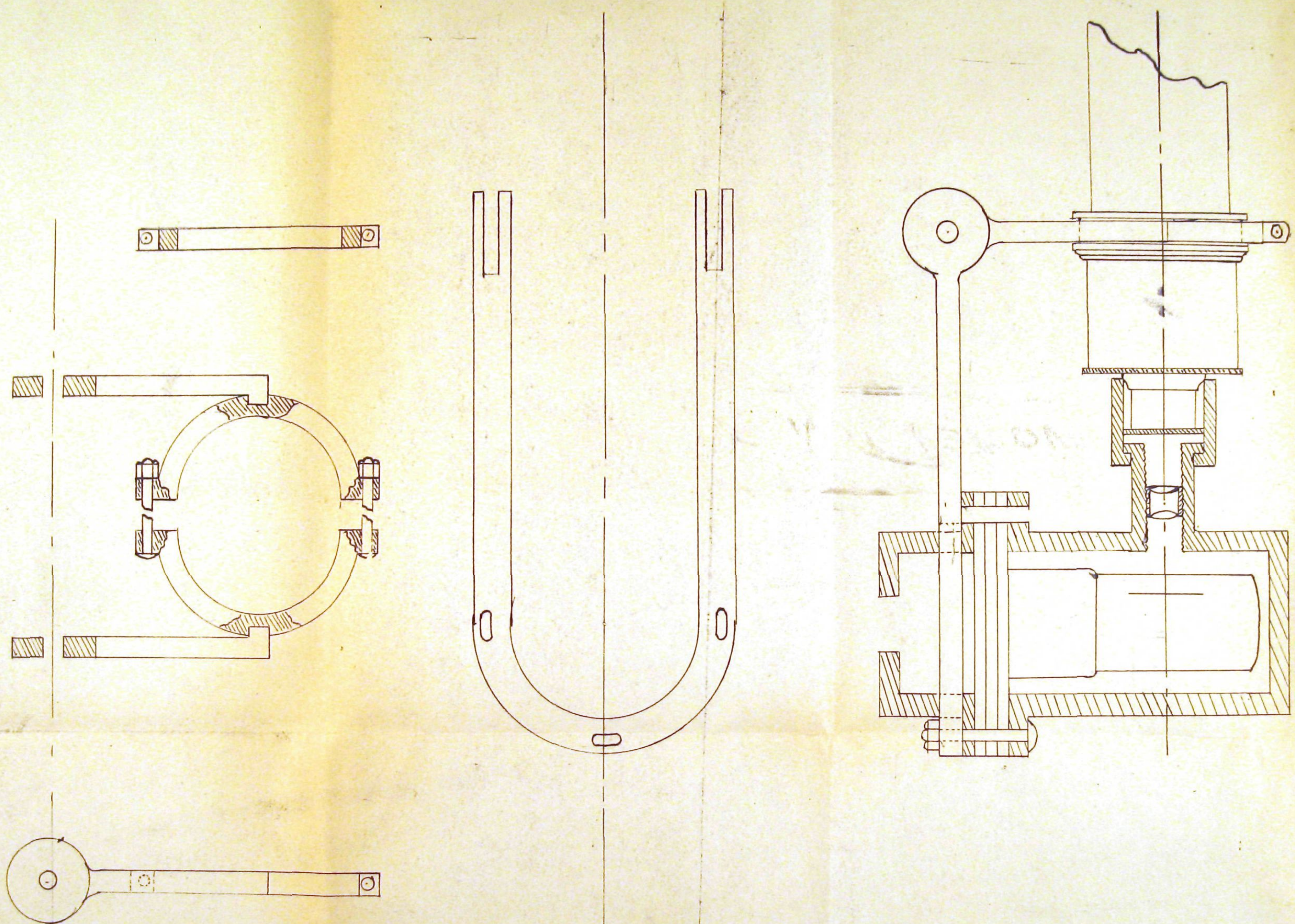

FIG 24

Fig 25

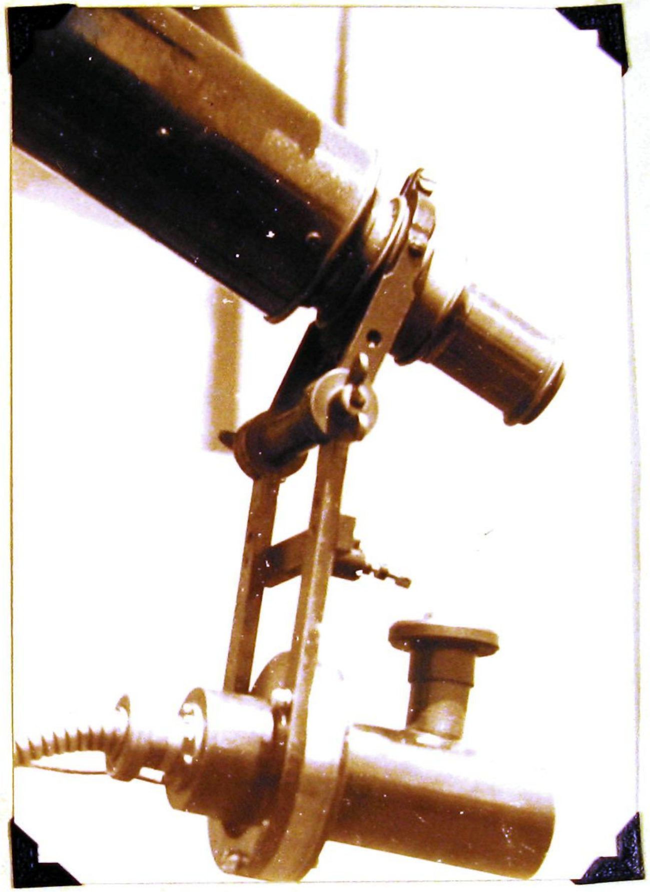

Fig 26

Fig 28

3. Stage Direct Coupled Amplifier

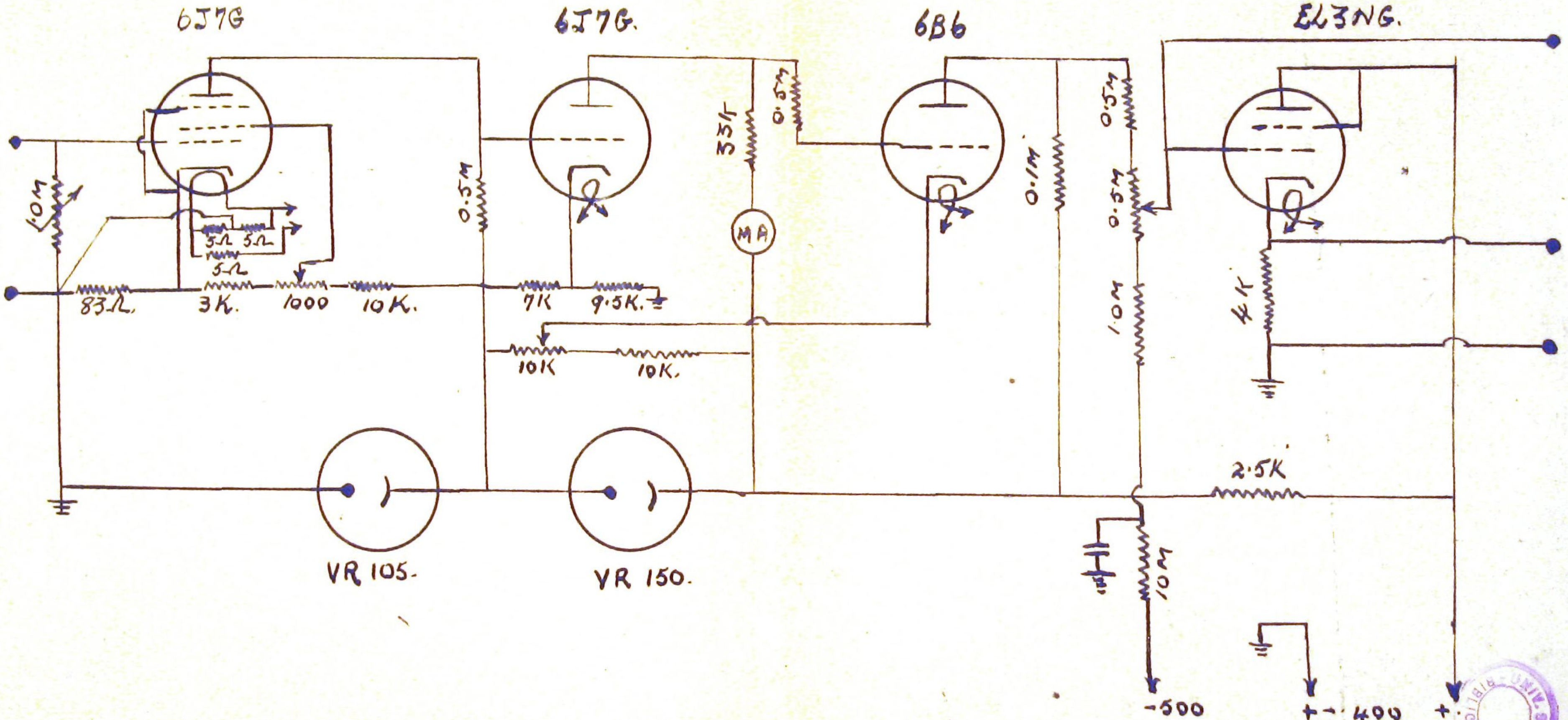

Fig 31

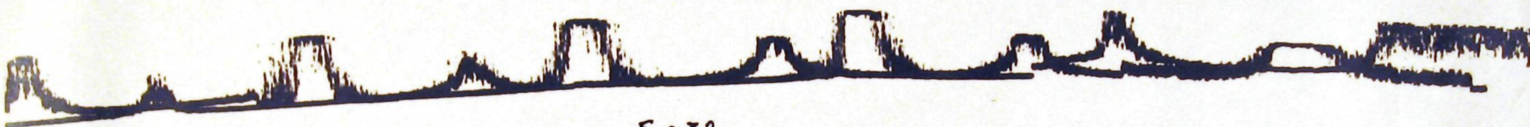

Fig 32

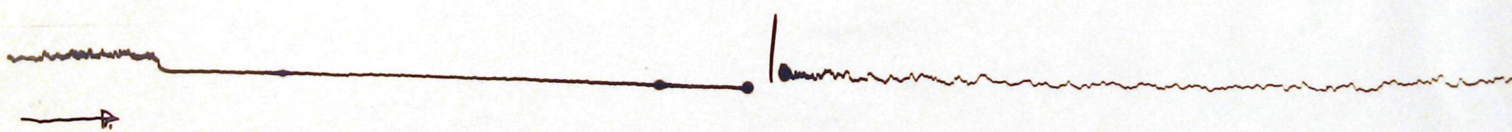

Fig 33

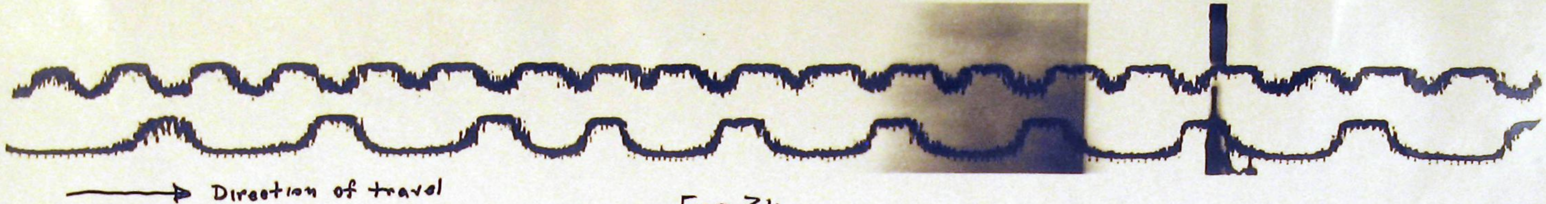

Fig 34

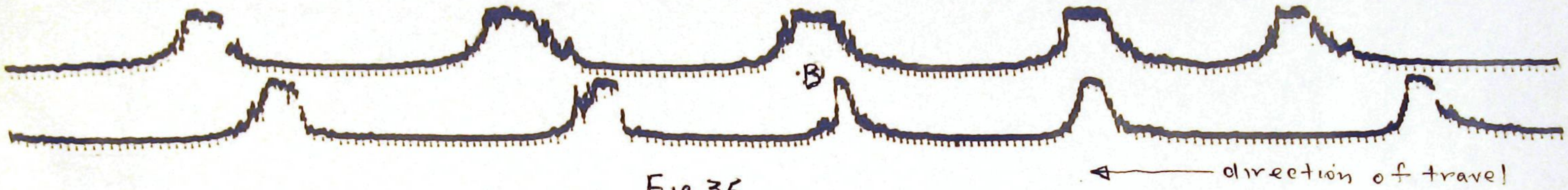

Fig 35

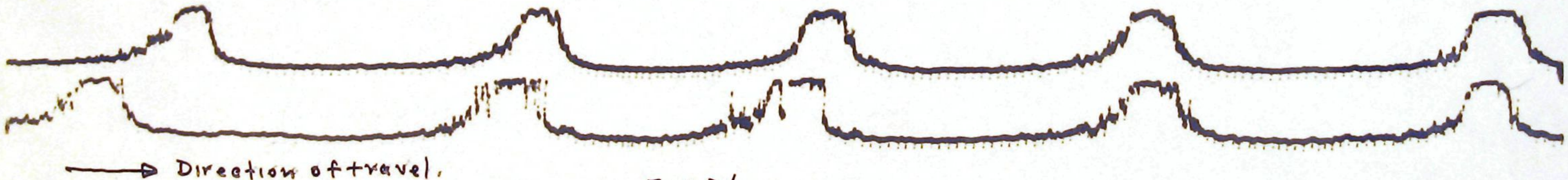

Fig 36

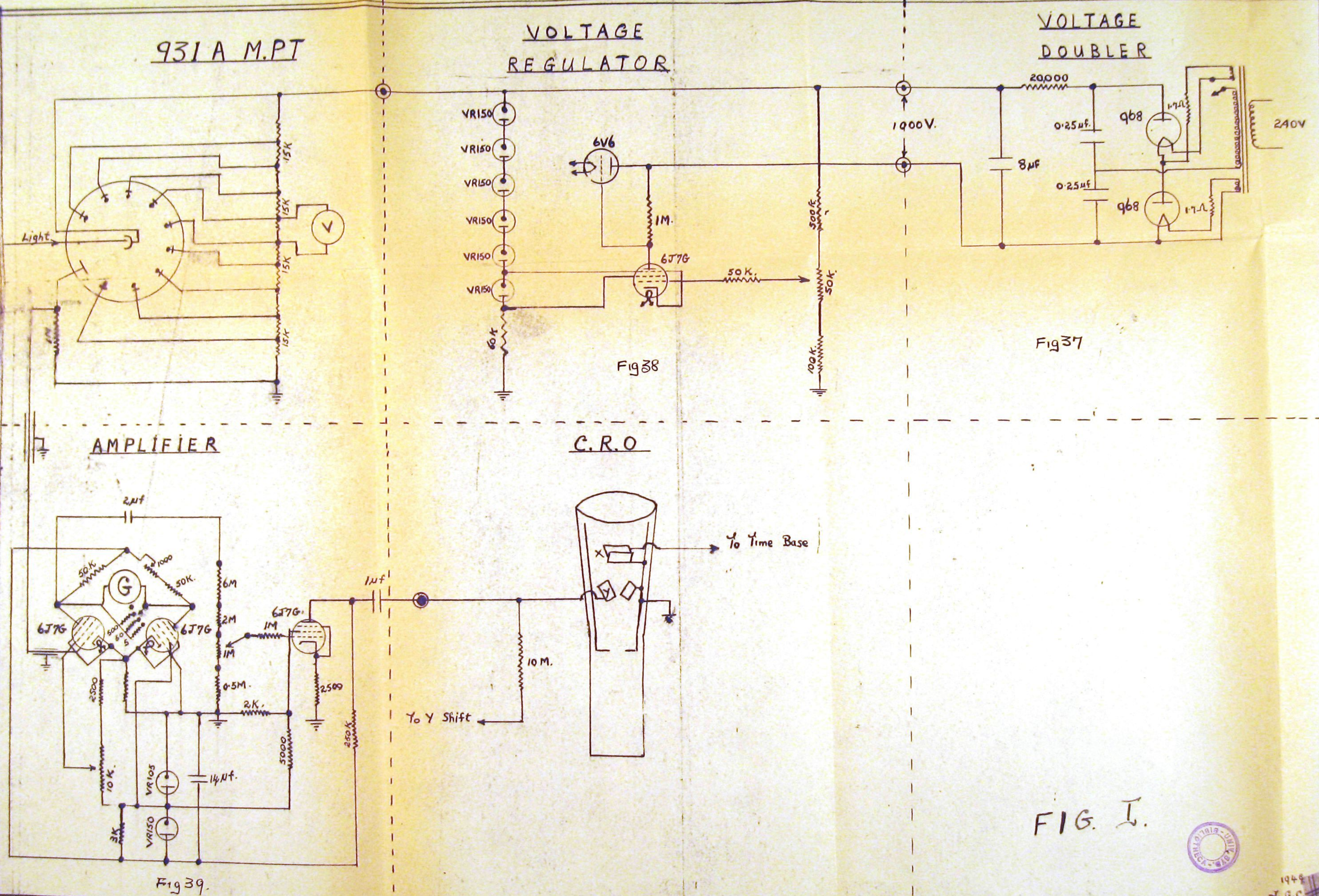
931 A M.PT
Light
15K
15K
15K
15K
VOLTAGE REGULATOR
VR150
VR150
VR150
VR150
VR150
VR150
60K
6V6
1M.
6J7G
50K.
500K.
50K.
100K.
Fig 38
VOLTAGE DOUBLER
1000V.
20,000
0.25µf.
0.25µf
8µf
968
968
240V
Fig 37
AMPLIFIER
2µf
50K
1000
50K.
G
6J7G
6J7G
500
6M
2M
1M
0.5M.
2K.
1M
6J7G.
2500
2500
5000
250K
10K.
VR105
14µf.
3K
VR150
Fig 39.
C.R.O
1µf
To Time Base
X
Y
10M.
To Y Shift
1948
J.G.C.

FIG. I.